

**NASA TECHNICAL
MEMORANDUM**

NASA TM X-64776

**CASE FILE
COPY**

**THE V-3 CONTAMINATION TEST OF THE CHAMBER A
FACILITY AND A SUBSEQUENT CRYOGENIC/VACUUM
STUDY OF THE V-3 TEST QUARTZ CRYSTAL MICROBALANCE**

**By W. Walding Moore, Jr., and Philip W. Tashbar
Space Sciences Laboratory**

March 30, 1973

NASA

*George C. Marshall Space Flight Center
Marshall Space Flight Center, Alabama*

EDITORS NOTE

Use of trade names or names of manufacturers in this report does not constitute an official endorsement of such products or manufacturers, either express or implied, by the National Aeronautics and Space Administration or any other agency of the United States government.

1. REPORT NO. NASA TM-X-64776		2. GOVERNMENT ACCESSION NO.		3. RECIPIENT'S CATALOG NO.	
4. TITLE AND SUBTITLE The V-3 Contamination Test of the Chamber A Facility and A Subsequent Cryogenic/Vacuum Study of the V-3 Test Quartz Crystal Microbalance *				5. REPORT DATE March 30, 1973	
				6. PERFORMING ORGANIZATION CODE	
7. AUTHOR(S) W. Walding Moore, Jr., and Philip W. Tashbar				8. PERFORMING ORGANIZATION REPORT #	
9. PERFORMING ORGANIZATION NAME AND ADDRESS George C. Marshall Space Flight Center Marshall Space Flight Center, Alabama 35812				10. WORK UNIT NO.	
				11. CONTRACT OR GRANT NO.	
12. SPONSORING AGENCY NAME AND ADDRESS National Aeronautics and Space Administration Washington, D. C. 20546				13. TYPE OF REPORT & PERIOD COVERED Technical Memorandum	
				14. SPONSORING AGENCY CODE	
15. SUPPLEMENTARY NOTES Prepared by Space Sciences Laboratory, Science and Engineering					
16. ABSTRACT <p>The areas of orbital and ground contamination of flight experiment hardware have been well established. This report relates directly to results of vacuum chamber testing for the ground evaluation of flight experiment hardware performance. First, the data obtained during the V-3 contamination testing in the Johnson Space Center's Chamber A space simulation test facility are presented. Second, during the V-3 contamination test, the MSFC Space Sciences Laboratory's quartz crystal microbalance exhibited two periods of anomalous readings. Therefore, a subsequent small chamber test was conducted in a controlled cryogenic/vacuum environment. The objective was to reproduce with known parameters the anomalous behavior patterns of the V-3 test data. Analyses of the anomalous readings are made on the basis of these tests. Additionally, as a by-product of the small chamber tests, calibration curves then existing for the quartz crystal microbalance were empirically extended, and certain data-formatting aids were documented.</p> <p>* The number V-3 is the Johnson Space Center's designation for the test to determine the contamination level of the Chamber A vacuum facility prior to the ATM thermal/vacuum simulation tests.</p>					
17. KEY WORDS vacuum testing cryogenic temperature contamination quartz crystal microbalance			18. DISTRIBUTION STATEMENT Unclassified - Unlimited <i>W. Walding Moore, Jr.</i>		
19. SECURITY CLASSIF. (of this report) Unclassified		20. SECURITY CLASSIF. (of this page) Unclassified		21. NO. OF PAGES 45	
				22. PRICE NTIS	

TABLE OF CONTENTS

	Page
I. INTRODUCTION	1
II. V-3 CONTAMINATION TEST DESCRIPTION	1
A. V-3 Contamination Test Purpose and Measurement Objectives	1
B. V-3 Contamination Test Instruments Configuration Description	2
C. QCM Operational Principles	6
D. Physical Description of Two-Piece QCM	6
E. Data Reduction and Discussion	7
III. CRYOGENIC/VACUUM STUDY DESCRIPTION	14
A. Purposes and Measurement Objectives	14
B. Test Instrumentation Descriptions	14
C. Test Procedures	17
D. Data Reduction and Discussion	18
IV. ANALYTICAL APPLICATION OF VACUUM STUDY TO V-3 TEST DATA	22
APPENDIX: REFERENCE INFORMATION, CHAMBER DATA AND SUPPORTING TEST DATA	27
REFERENCES	38

LIST OF ILLUSTRATIONS

Figure	Title	Page
1.	Closeup view of the QCM test configuration for the V-3 Contamination Test	3
2.	Quadrupole RGA head mounted to view RTCM mirror	4
3.	Data acquisition equipment for SSL V-3 test sensors	4
4.	Exploded view of the two-piece QCM.	5
5.	QCM data, V-3 Contamination Test, July 12, 1971	9
6.	QCM data, V-3 Contamination Test, July 13, 1971	9
7.	QCM data, V-3 Contamination Test, July 14, 1971	10
8.	QCM data, V-3 Contamination Test, July 15, 1971	10
9.	QCM data, V-3 Contamination Test, July 16, 1971	11
10.	V-3 test data for QCM beat frequency, temperature analog, and Chamber A pressure as functions of time for first anomalous period	12
11.	V-3 test data for QCM beat frequency, temperature analog, and Chamber A pressure as functions of time for second anomalous period	13
12.	Closeup view of instrumented QCM and conductive mount for chamber installation	15
13.	Closeup side view of instrumented QCM and conductive mount for chamber installation	15
14.	Schematic view of the two-piece QCM, including sensors locations for the cryogenic/vacuum test	16
15.	View of chamber configuration for cryogenic/vacuum study	17

LIST OF ILLUSTRATIONS (Concluded)

Figure	Title	Page
16.	Overall view of laboratory setup for cryogenic/vacuum study	18
17.	Block diagram of the QCM test configuration for the cryogenic/vacuum study	19
18.	Cryogenic/vacuum study test data for QCM beat frequency, temperature analog, crystal housing thermistor, crystal housing thermocouple, shroud thermocouple, and chamber pressure as functions of time.	20
19.	Cryogenic/vacuum study test data for QCM beat frequency, temperature analog, electronics housing thermistor, electronics housing thermocouple, shroud thermocouple, and chamber pressure as functions of time	21
20.	Cryogenic/vacuum study ventings test data for QCM beat frequency, temperature analog, shroud thermocouple, and chamber pressure as functions of time	23
A-1.	Data graphical summary for the pre-test radiatively-cooled cryogenic/vacuum performance check	29
A-2.	Calibration curve for temperature analog voltage output versus temperature for the range +120° to -65°C	30
A-3.	Calibration curve for beat frequency output versus temperature for the range +120° to -65°C	31
A-4.	Representative manufacturer (Atlantic Research Corporation) calibration curves for temperature analog shift thermal dependencies	32
A-5.	Representative manufacturer (Atlantic Research Corporation) calibration curves for beat frequency shift thermal dependencies	33

LIST OF TABLES

Table	Title	Page
1.	QCM Testing Connections and Functions	7
2.	Sequence of Test Events During the Venting Periods	25
A-1.	Thermocouple/Thermistor Data Chart	34
A-2.	Temperature Analog Conversion Data	36

THE V-3 CONTAMINATION TEST OF THE CHAMBER A FACILITY AND A SUBSEQUENT CRYOGENIC/VACUUM STUDY OF THE V-3 TEST QUARTZ CRYSTAL MICROBALANCE

I. INTRODUCTION

The areas of orbital and ground contamination of flight experiment hardware have been established, as evidenced by References 1 and 2.

II. V-3 CONTAMINATION TEST DESCRIPTION

A. V-3 Contamination Test Purpose and Measurement Objectives

During July 1971, a ground-based contamination measurements team instrumented the Johnson Space Center's (JSC) large vacuum facility (Chamber A). The purpose was to determine quantitatively and qualitatively the degree of cleanliness during chamber operation. One of the instrumentation systems was a joint effort of the Naval Research Laboratory (NRL) and the Marshall Space Flight Center's (MSFC) Space Sciences Laboratory (SSL). The SSL subsystem consisted of a quartz crystal microbalance (QCM), a quadrupole residual gas analyzer (RGA), an ionization vacuum gauge, and a free air thermocouple. The test objectives for these instruments were as follows:

1. Determine quantitatively and qualitatively the residual gas background in the test location area of Chamber A,
2. Measure deposition and re-evolvment of contaminants at determined pressures and temperatures,
3. Time-line contamination events taking place on the NRL real-time contamination monitor (RTCM) with the RGA and the QCM, and
4. Monitor the operational performance of Chamber A during initial pumpdown, thermal-vacuum operation, and repressurization.

One test requirement specified that the chamber pressure was to be held at 1×10^{-6} torr for a period of 70 hours minimum. This was amended during the test to 2×10^{-6} torr because of leaks from the chamber exterior. All the liquid nitrogen panels as well as the lunar plane were to be cooled by liquid nitrogen (LN_2) to 100°K or lower. A minimum of five gaseous helium panels were to be cooled to approximately 20°K. Gaseous nitrogen (GN_2) was used for the repressurization cycle of the test.

The top sun and an IR cage provided the solar simulation for this test. They were operated for 20 hours in cyclic operation of 1 hour on and 0.5 hour off, 20 hours of continuous burn, and 30 hours of infrared (IR) cage on with top sun off. The contamination limits for this test specified that during the 40 hours of solar operation, NRL's RTCM should show no more than 5 percent reflectance loss when monitoring with a light source of the Lyman-Alpha wavelength of hydrogen. For the total test of 70 hours, this RTCM was not to exceed 10 percent total reflectance loss.

The cleaning procedure for the interior of the chamber, prior to the test, included cleaning the side and top sun with Freon. The chamber was cleaned with deionized water and Penn-6 from the 2.438-m (8-ft) level to the bottom of the plenum, and all chamber surfaces were cleaned with deionized water. In addition, chamber surfaces exhibiting 3×10^{-7} g/cm² of contamination were cleaned with Freon.

B. V-3 Contamination Test Instruments Configuration Description

Figures 1, 2, and 3 give the overall picture of the instrumentation system configuration. The NRL RTCM's are in the upper left of Figure 1. The SSL subsystem is located in the center right of the photograph. The entire system is mounted on a 5.79-m (19-ft) test stand positioned on the lunar plane level of Chamber A. The SSL subsystem is facing the center of the chamber. The NRL monitors are oriented toward the solar simulation lamps in the chamber top. Figure 2 shows the RGA mounting detail with the unit's ion source viewing directly the RTCM mirror for evaluating any re-evolving contaminants during heating of the mirror. The data acquisition equipment is depicted in Figure 3. From left background to right foreground, the consoles are: the Process Analyzers, Inc. (PAI) quadrupole RGA system, the x-y analog recording system, a Hewlett-Packard Model 2010 data acquisition system, and a Hewlett-Packard Model 2114 computer analysis system. By referring to Figure 4, the QCM sensor can be determined. In addition, the ionization gauge is located next to the QCM coaxial tubes. The RGA head is positioned at the top end of the center NRL RTCM such that it views the sensing optical surface.

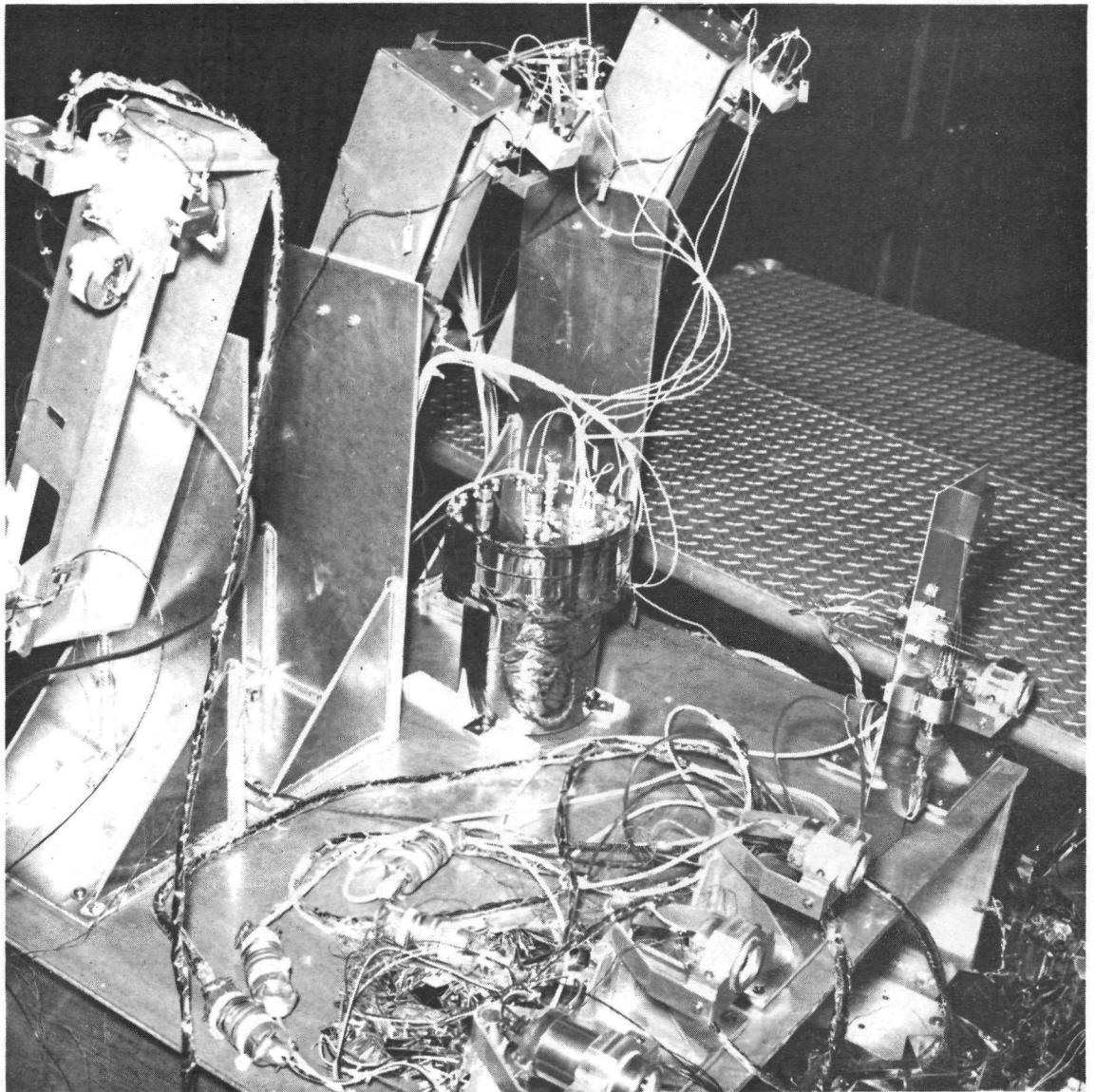


Figure 1. Closeup view of the QCM test configuration for the V-3 Contamination Test.

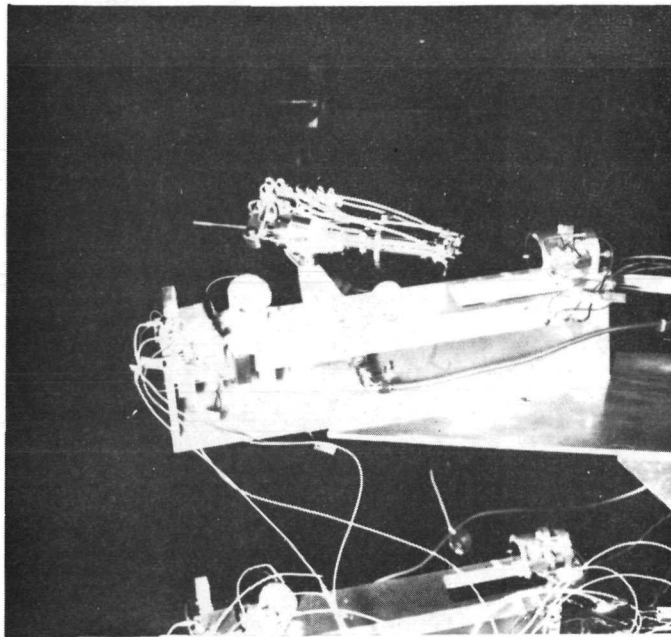


Figure 2. Quadrupole RGA head mounted to view RTCM mirror.

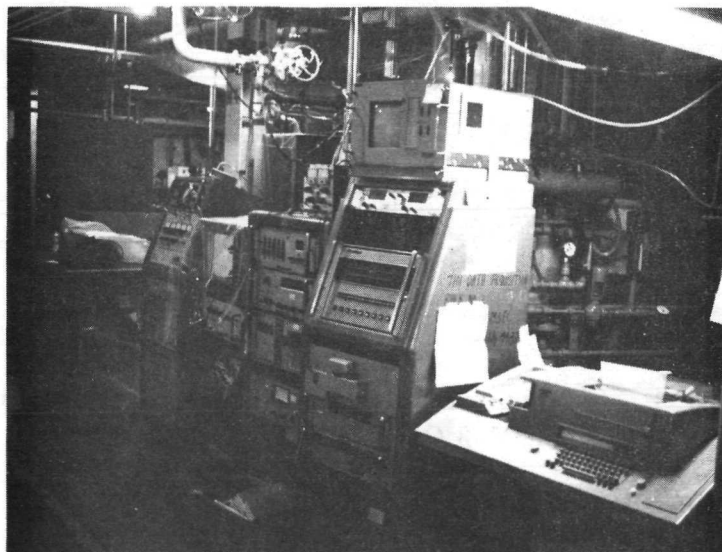


Figure 3. Data acquisition equipment for SSL V-3 test sensors.

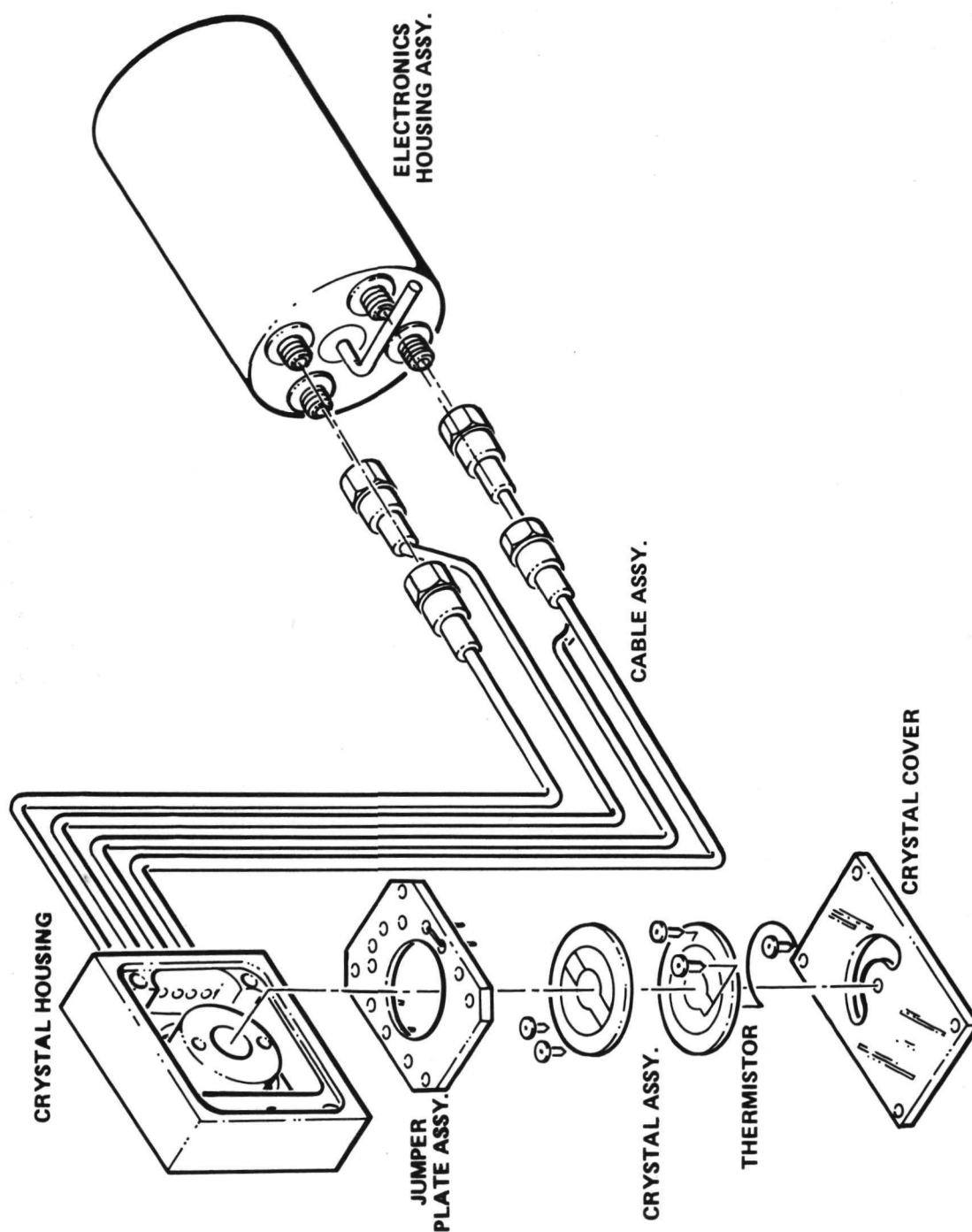


Figure 4. Exploded view of the two-piece QCM.

Unfortunately, during this test, the quadrupole RGA was inoperative because of a shorted filament in the ion source. Consequently, this report will concentrate on the other data sensors.

C. QCM Operational Principles

This report is primarily concerned with the interpretation of readings produced by the QCM during the Chamber-A, V-3 Contamination Test. The Atlantic Research Corporation of Costa Mesa, California, designed and built the two-piece, flight prototype QCM used in the V-3 Contamination Test. The sensing element of the unit consists of two nearly identical AT-cut (small frequency shifts with temperature) quartz crystal plates, each operating at approximately 10 MHz. The crystal plates are mounted between metal rings to minimize their relative thermal gradient. One crystal plate, called the sensing crystal, operates with its active electrode area exposed to the environment to be monitored. The remaining crystal plate, called the reference crystal, is shielded by the mounting configuration and housing from the environment. A thermistor, located on the reference side of the metal ring, monitors the crystal temperature. This output will subsequently be called the temperature analog. The operating frequencies of the reference and sensing crystals are difference processed, producing an audio range frequency, called the beat frequency, which is set to shift upwards in magnitude as mass deposits on the sensing crystal.

D. Physical Description of Two-Piece QCM

The two-piece QCM that is used has the sensor assembly separated from the electronics package. The electronics is contained in a hermetically-sealed, argon-filled stainless steel cylinder to prevent self-contamination of the sensor assembly. The sensor assembly is contained in a stainless steel box. The sensing crystal is recessed 0.01 m in the housing. The environment viewing opening is 0.006 m in diameter. The back plate contains a venting groove to prevent relative pressurization of the chamber volume around the reference crystal. The two subsystems are connected by coaxial cable copper tubes. Details of the QCM test connections and functions are contained in Table 1. Further information on the instrumentation and V-3 Contamination Test can be found in References 3 and 4. One point for later reference should be made: The QCM system used was composed of the crystal assembly of unit S/N 002 and the electronics package of unit S/N 004.

TABLE 1. QCM TESTING CONNECTIONS AND FUNCTIONS

Pins	Data Number	Connections	Functions
A	2	0 to 5 Vdc Crystal Temperature Analog	Nonlinear crystal temperature monitor
B	-	Common	For one functional output
C	-	Common	For one functional output
D	-	28 Vdc Primary Input Power	Electronics package power
E	1	0 to 5 Vdc Mass Analog	Mass deposition monitor; sensitivity 0.45 mV/Hz
F	-	Common	For one functional output
G	-	Common	For one functional output
H	3	10 to 15 V, Peak-to-Peak Beat Frequency Waveform	Mass deposition monitor by frequency shift
J	-	Common	Structure ground
K	-	None	No function

E. Data Reduction and Discussion

The pumpdown of Chamber A began at 1200 hrs on July 12, 1971. Figures 5 through 9 are graphs of QCM frequency, thermistor temperature of the reference crystal, and pressure of the chamber versus time of the test. At approximately 1944 hrs (Fig. 5), cryopumping in the chamber began. At 1947 hrs, diffusion pump 2 was brought on line.

On July 13, 1971, at 0151 hrs (Fig. 6), three additional diffusion pumps were brought on line. At 0250 hrs, the heaters were activated on the nitrogen purge line attached to the ATM canister. For this latter event, the QCM detected 10^{-3} grams of contaminants that had a stay time of 3 hours. Since the QCM's operation was saturated for this event and later returned to its normal operating frequency, water is believed to be the contaminant. This is based on temperature profiles analysis.

At 0600 hrs, the top sun and the IR cage in the chamber were turned on for 20-hour solar simulation consisting of 1-hour periods with the sun on and 0.5-hour periods with the sun off. At this time, the water vapor evolved from the QCM's crystal surface. This 20-hour solar cycling operation ended at 0130 hrs on July 14, 1971. Note in Figure 6 the tracking of the QCM frequency with the change in thermistor temperature because of the solar cycling.

On July 14, 1971, at 0200 hrs (Fig. 7), the IR cage and the top sun were switched on for a 20-hour continuous burn. Beginning at approximately 1200 hrs, the QCM detected, in a span of 2 hours, contaminants of 4.6×10^{-6} , 5.5×10^{-6} , and 5.8×10^{-6} grams, respectively. The average stay time for these contaminants was 0.5 hour. Note that the thermistor temperature was stable for this period of the test. No correlation with chamber events has been made at this time. At 2200 hrs, the cold soak phase of the test began.

At 0030 hrs on July 15, 1971 (Fig. 8), 3×10^{-6} grams of contaminants were deposited on the QCM and had a stay time of 30 minutes. The spikes on the pressure curve are caused by inert gases being purged through an ultra-violet source that was being calibrated inside the chamber. These gases included helium and a helium-neon mixture.

On July 16, 1971, at 0400 hrs (Fig. 9), the diffusion pumps were turned off and the chamber warmup sequence began. At 0420 hrs, heating of the lunar plane was initiated. In-bleed of warm nitrogen was started at 0612 hrs to bring the chamber pressure up to about 4 torr. At this time, the QCM became saturated and stopped oscillating for 6 hours. The IR cage was turned on to one-third maximum at 0603 hrs, and at 0725 hrs, the lunar plane reached a temperature of 280°K (44°F). At 1750 hrs, the nitrogen in-bleed was increased. Note the spike on the QCM frequency curve for this event.

In general, the QCM monitoring of the V-3 Chamber A Contamination Test was relatively straightforward except for the anomalous data periods on July 13 and 16, 1971. All contaminant deposits which occurred did not appear to be of polymeric materials origin. The next section of this report will examine the causes of the anomalous data which have been replotted for clarity in Figures 10 and 11.

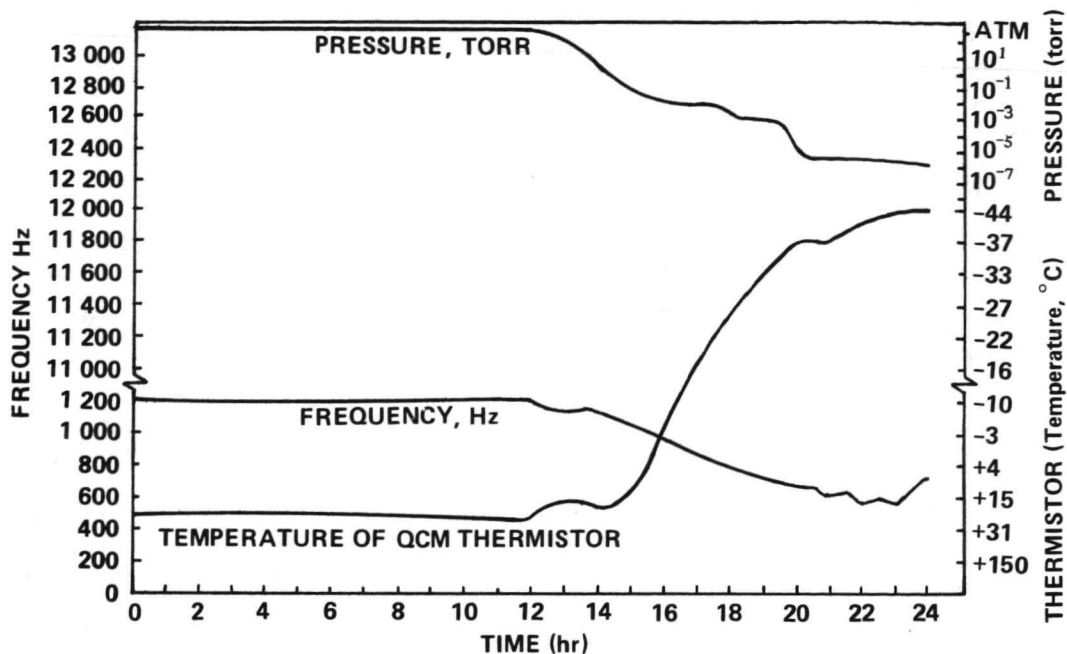


Figure 5. QCM data, V-3 Contamination Test, July 12, 1971.

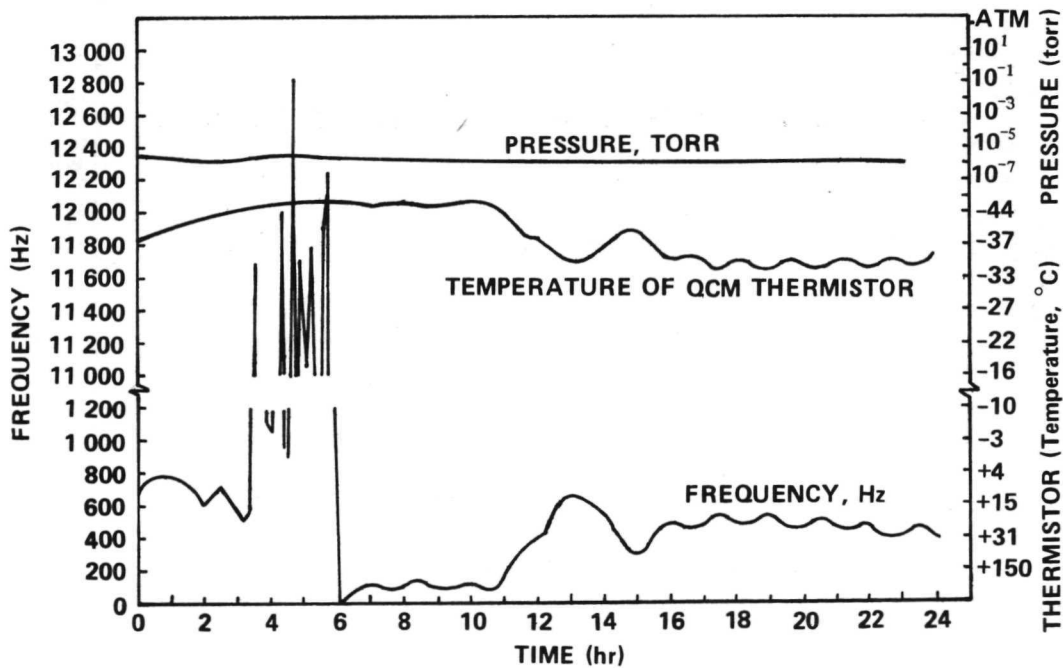


Figure 6. QCM data, V-3 Contamination Test, July 13, 1971.

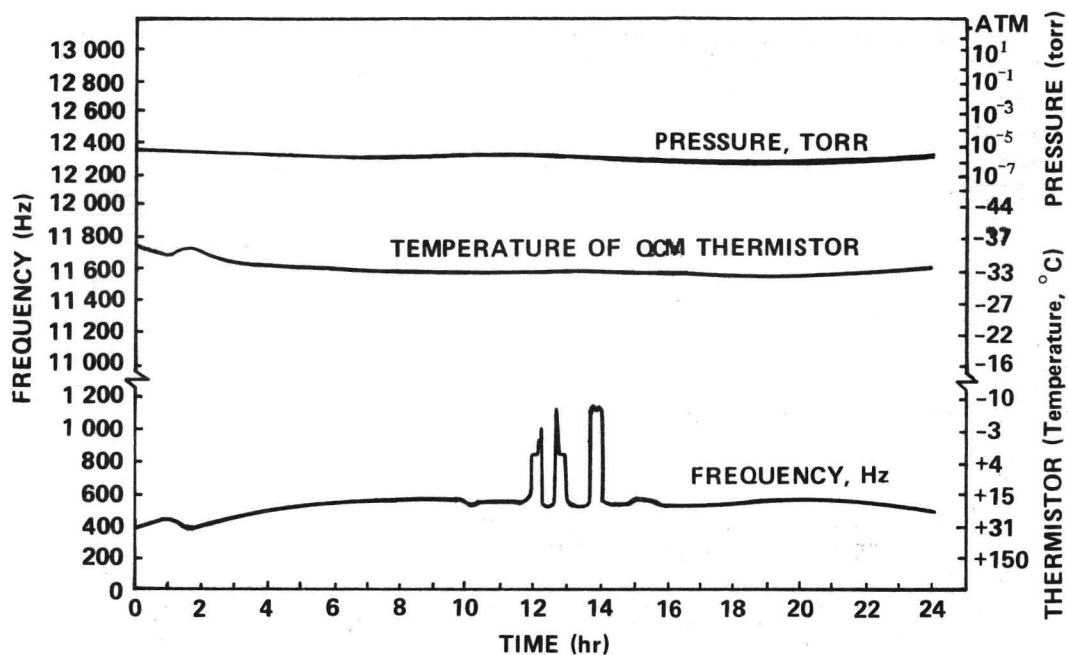


Figure 7. QCM data, V-3 Contamination Test, July 14, 1971.

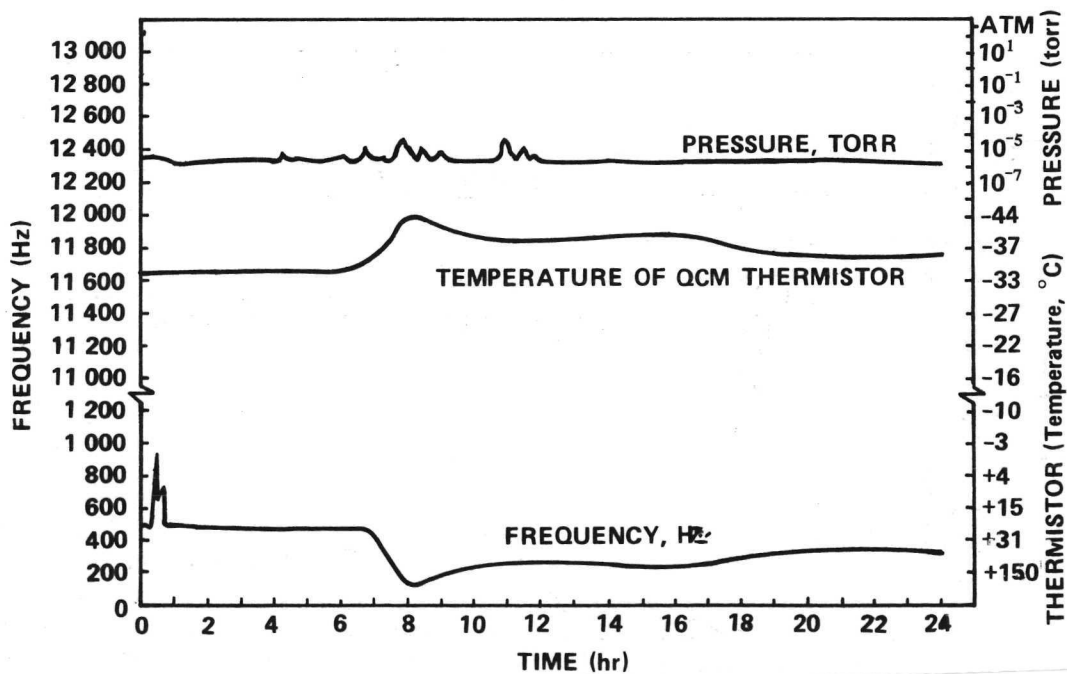


Figure 8. QCM data, V-3 Contamination Test, July 15, 1971.

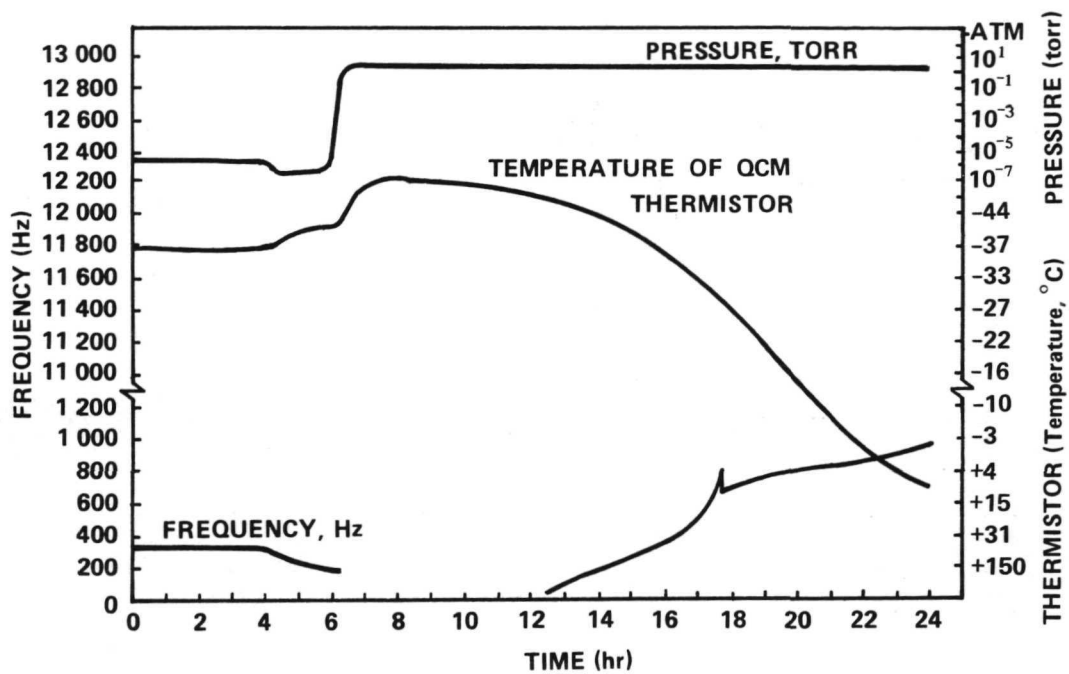


Figure 9. QCM data, V-3 Contamination Test, July 16, 1971.

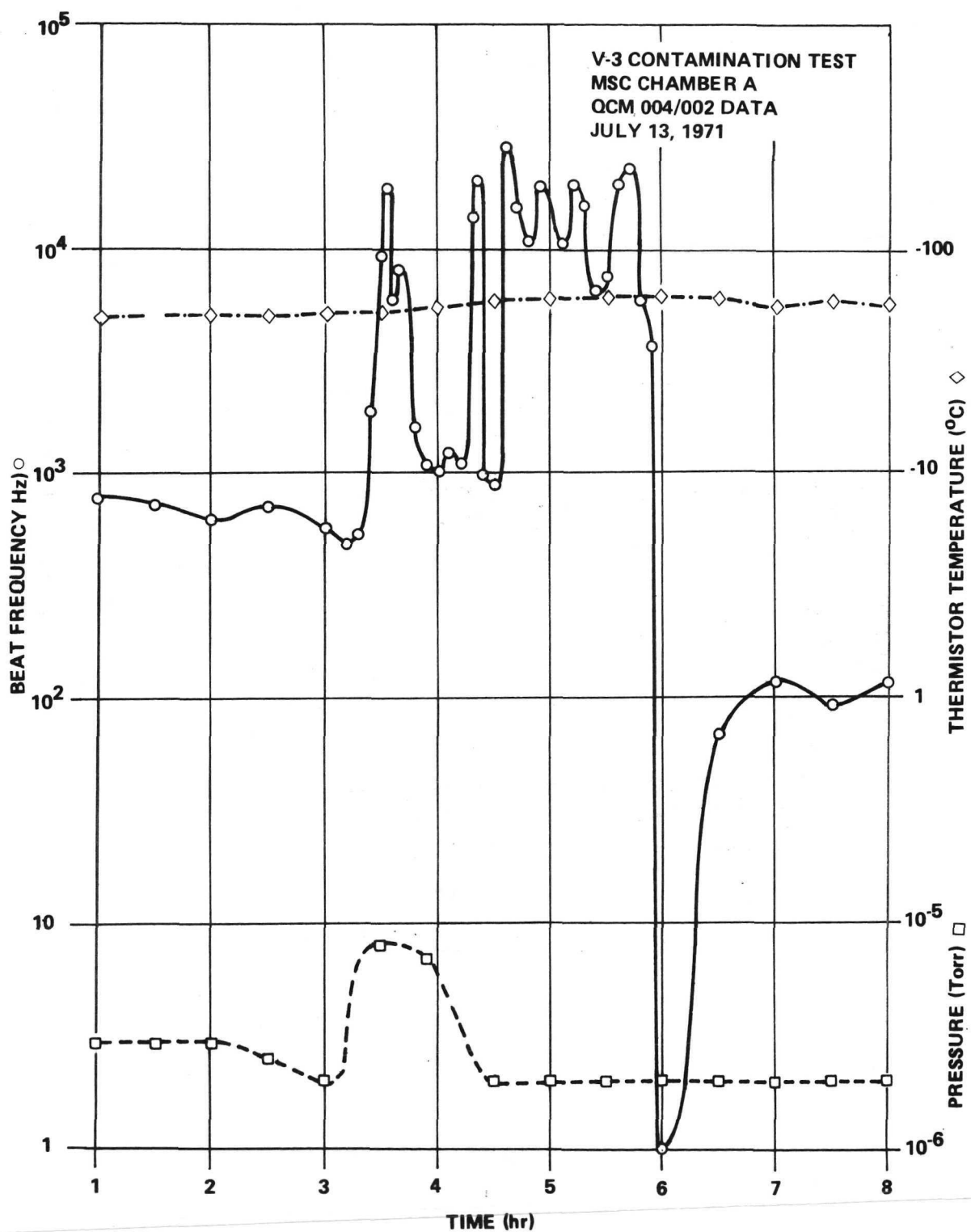


Figure 10. V-3 test data for QCM beat frequency, temperature analog, and Chamber A pressure as functions of time for first anomalous period.

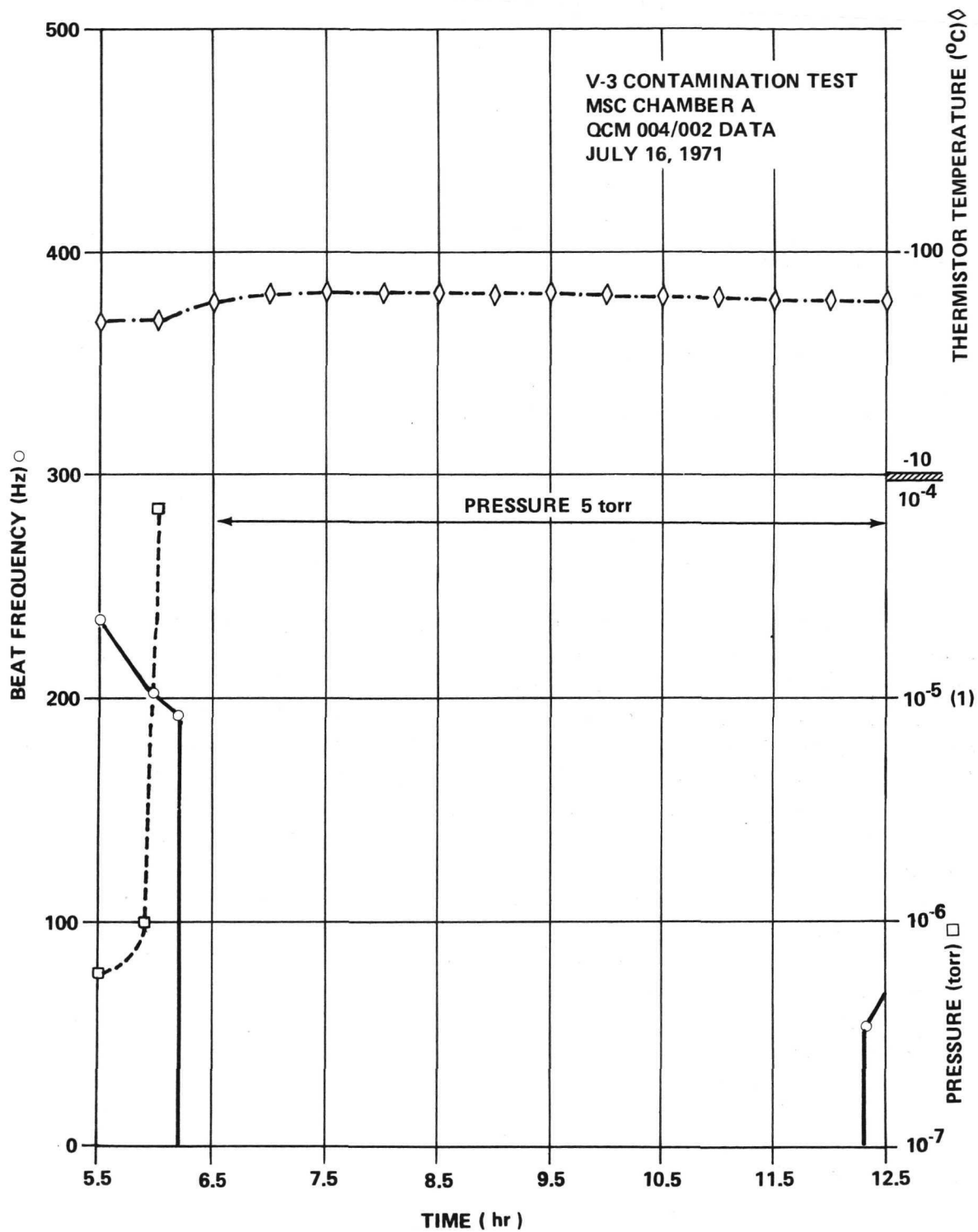


Figure 11. V-3 test data for QCM beat frequency, temperature analog, and Chamber A pressure as functions of time for second anomalous period.

III. CRYOGENIC/VACUUM STUDY DESCRIPTION

A. Purposes and Measurement Objectives

During the described V-3 Contamination Test of JSC Chamber A, two particular periods of anomalous QCM readings (Figs. 10 and 11) were recorded. The primary purpose of this cryogenic/vacuum study was to establish the nature of these readings; that is, to determine if the instrument output was caused by external noise, electronics problems, crystal oscillation mismatch problems, or data. In addition, because of the variation of beat frequency with temperature in the limits of and outside of design ranges, a secondary goal was set to produce empirical calibration curves for the beat frequency and the temperature analog. To achieve the study goals, the V-3 test QCM was instrumented for crystal and electronics housing temperatures and operated in a cryogenic vacuum.

B. Test Instrumentation Descriptions

Using Figures 12, 13, and 14, we can describe the QCM mounting and sensor locating details for the cryogenic/vacuum study. The mounting technique duplicates, within reason, the Chamber-A mount. However, this mount was designed for conductive cooling to the liquid nitrogen (LN_2) liner. The cooling of the QCM during the V-3 test was through radiation to the Chamber-A gaseous helium shrouds. A restricted test procedure was executed using a radiative cooling mount (Fig. A-1 of appendix). These results were used to check instrument readout repetition and the mounting simulation of conductive cooling. In Figures 12, 13, and 14 the positions of the crystal and electronics housings' thermistors are visible. Note that the thermal contact was assured by mechanical pressure during the time the vacuum-rated epoxy was hardening. Also, during the entire test, even under heat lamp irradiation, the QCM gave no indication of the material outgassing. In Figures 12 and 13 the darker area which leads to the crystal and electronics housings' copper-constantan thermocouples may be determined after study of Figure 14 for their positions. Specifically, the thermocouples are held in contact by the mounting mechanical pressure directly opposing the corresponding thermistor. In addition, Figures 12 and 13 show the power and data conductor bundle and functional feedthrough arrangement. The details of the feedthrough arrangement will be associated with Figure 15.

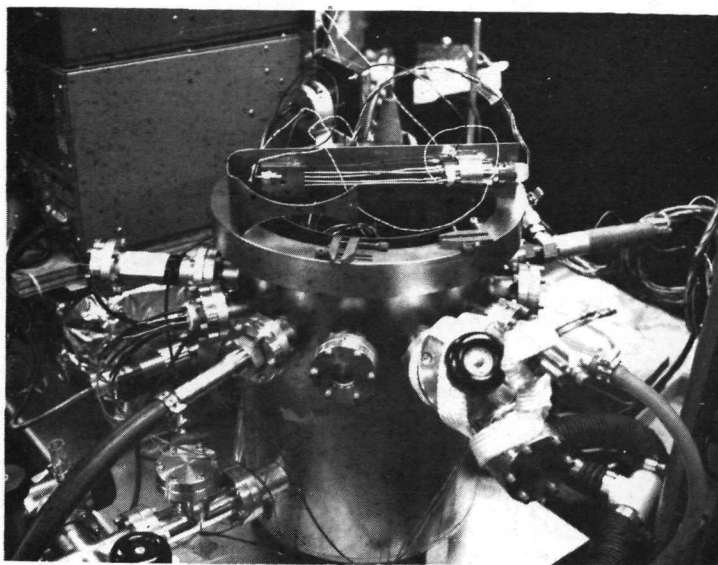


Figure 12. Closeup view of instrumented QCM and conductive mount for chamber installation.

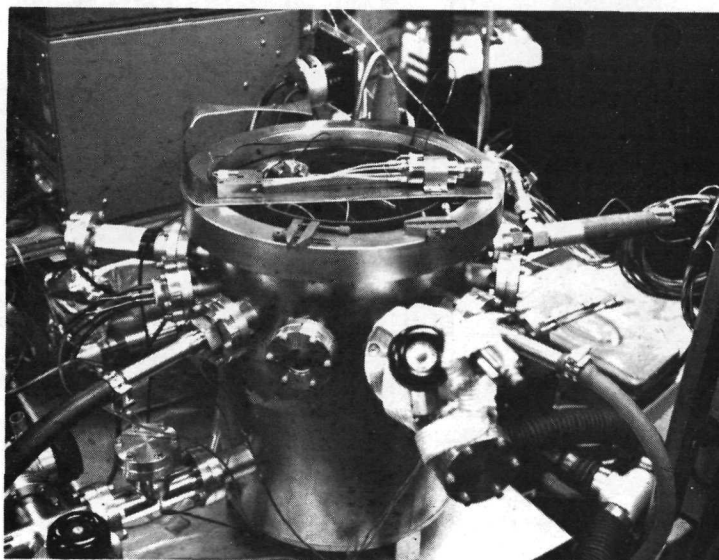


Figure 13. Closeup side view of instrumented QCM and conductive mount for chamber installation.

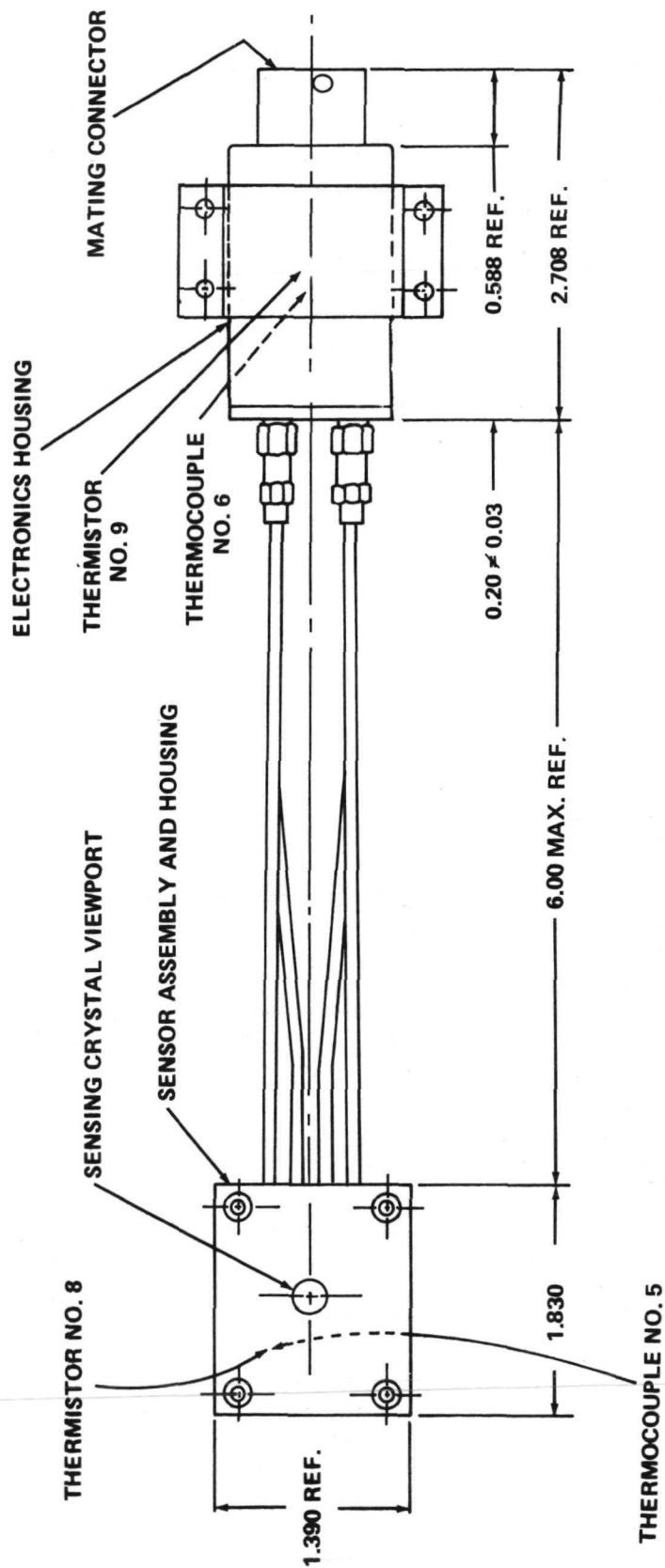


Figure 14. Schematic view of the two-piece QCM, including sensors locations for the cryogenic/vacuum test.

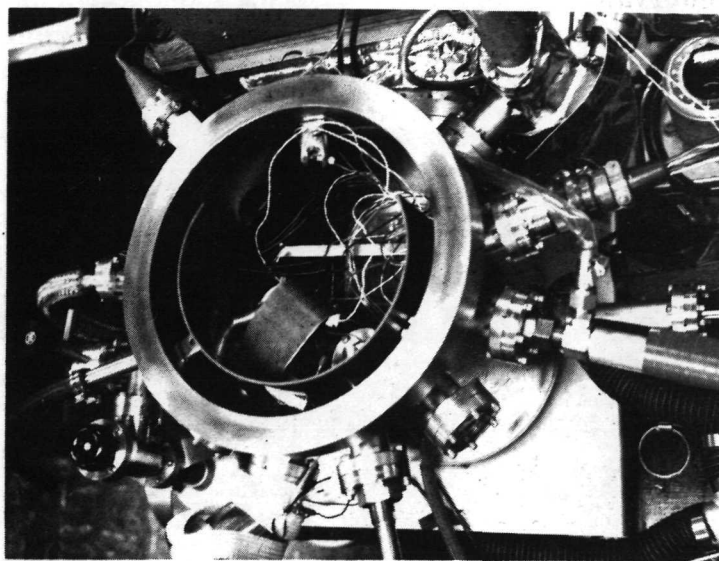


Figure 15. View of chamber configuration for cryogenic/vacuum study.

In Figure 15, the QCM mounting unit is seen installed in the vacuum chamber with the copper plate mount clamped to the cylinder-portion LN₂ liner. The top of the QCM crystal housing is visible as the lighter area. The position of the shroud thermocouple is directly opposite the crystal housing that is clamped to the LN₂ liner. Beginning with the feedthrough toward the upper right corner and reading counterclockwise, the chamber feedthrough ring is utilized as follows: pressure gauge, LN₂ liner outlet (combination mechanical and sorption forepump system visible beneath), viewport, sample inlet port, LN₂ liner inlet, viewport, mechanical feedthrough (thermistors feedthrough visible beneath), power and data electrical feedthrough, and partial pressure gauge. The overall view of the setup in Figure 16 shows the chamber with the digital data acquisition system in the left foreground and the thermistor read-out system in the right background. Finally, Figure 17 shows the system in block diagram form with the individual measurements numerically labeled in the order of their acquisition by the data systems.

C. Test Procedures

The testing sequence followed in this study included an ambient condition check period, a vacuum pumpdown period, a cryogenic cool-down period, a brief cryogenic hold period, and a samples venting period. During all periods,

the primary mode of data acquisition was 1-minute intervals with 10-second and 10-minute intervals as appropriate. During the ambient check, after all instrumentation had been warmed up and calibrated, the system was monitored near atmospheric pressure and room temperature. The vacuum pumpdown was achieved by, first, trapped mechanical and then sorption pumping in the 10^{-3} torr range.

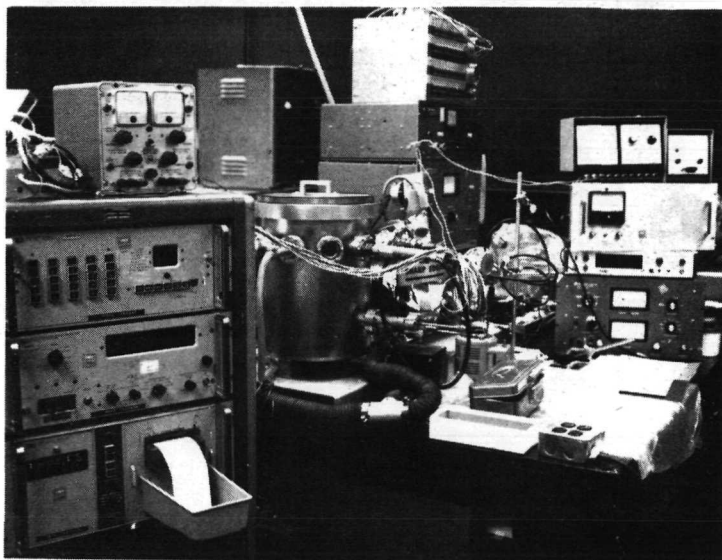


Figure 16. Overall view of laboratory setup for cryogenic/vacuum study.

The cryogenic cool-down transition was achieved by filling the LN_2 liner and keeping it continuously topped out. The cryogenic hold period was achieved by using a heat lamp to produce a dynamic thermal balance at about the desired point. Because of this necessity, the long cryogenic hold period of the V-3 test could not be simulated. The sequence and number of samples vents, produced by quickly opening and closing the isolation valve, was laboratory air (4), alcohol (2), water (valve remaining open) and laboratory air (3).

D. Data Reduction and Discussion

To facilitate achieving the secondary goal, the data generated have been reduced and presented in the survey shown in Figures 18 and 19. Figure 18 concentrates on the crystal housing, and Figure 19 concentrates on the electronics housing. Because reducing voltage data for temperature is time-consuming, a composite conversion working chart, which may be of further

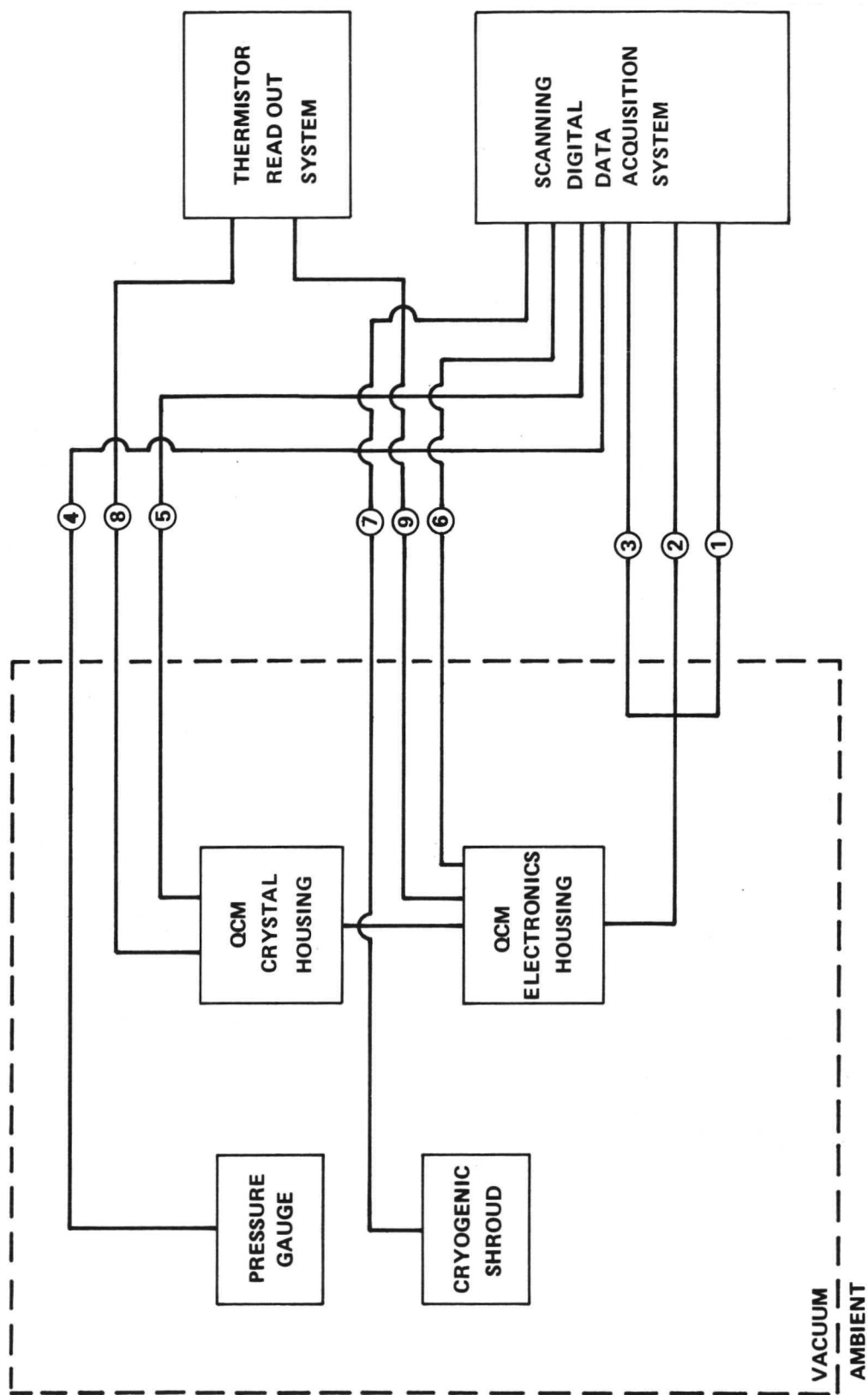


Figure 17. Block diagram of the QCM test configuration for the cryogenic/vacuum study.

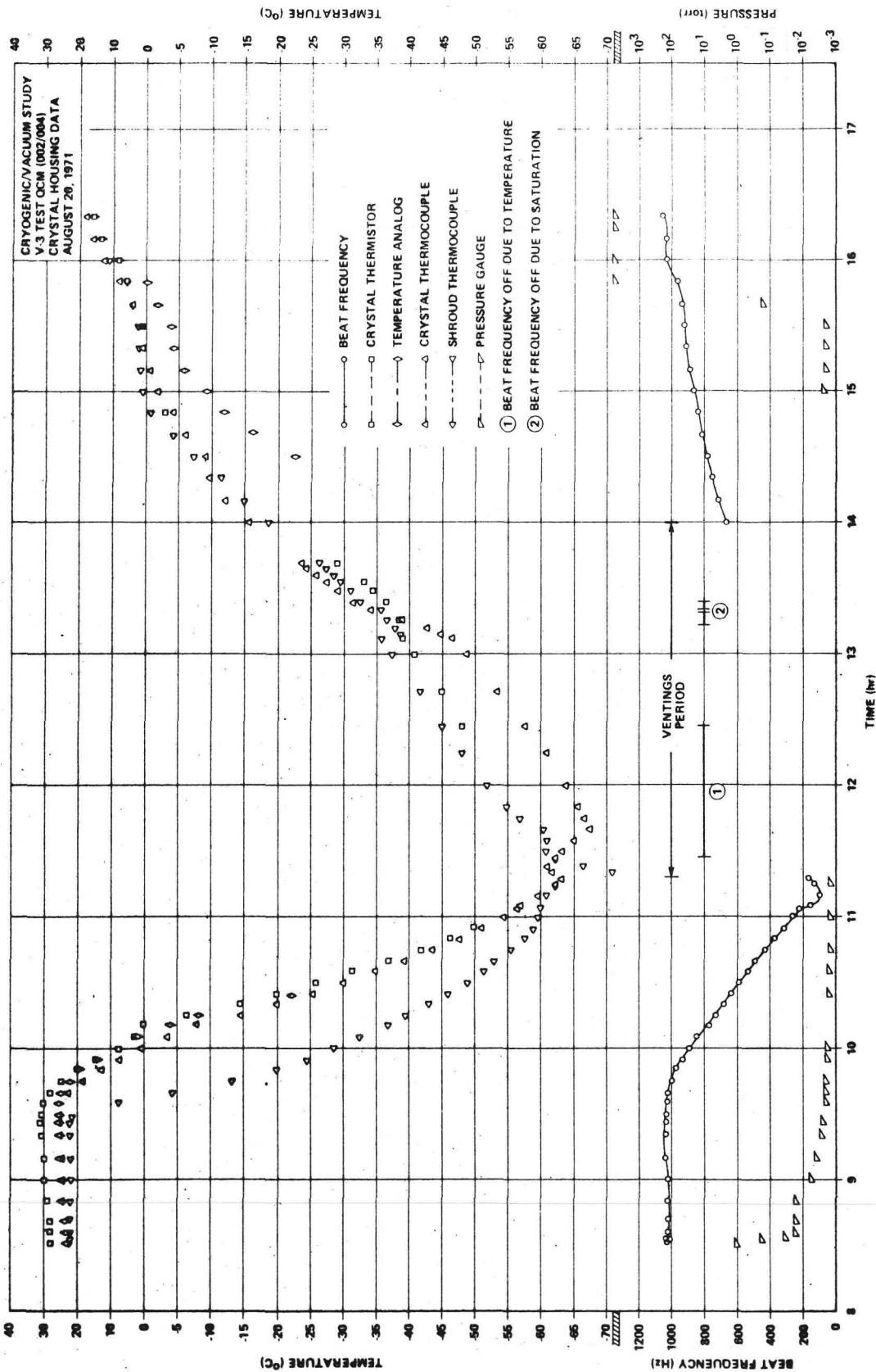


Figure 18. Cryogenic/vacuum study test data for QCM beat frequency, temperature analog, crystal housing thermistor, crystal housing thermocouple, shroud thermocouple, and chamber pressure as functions of time.

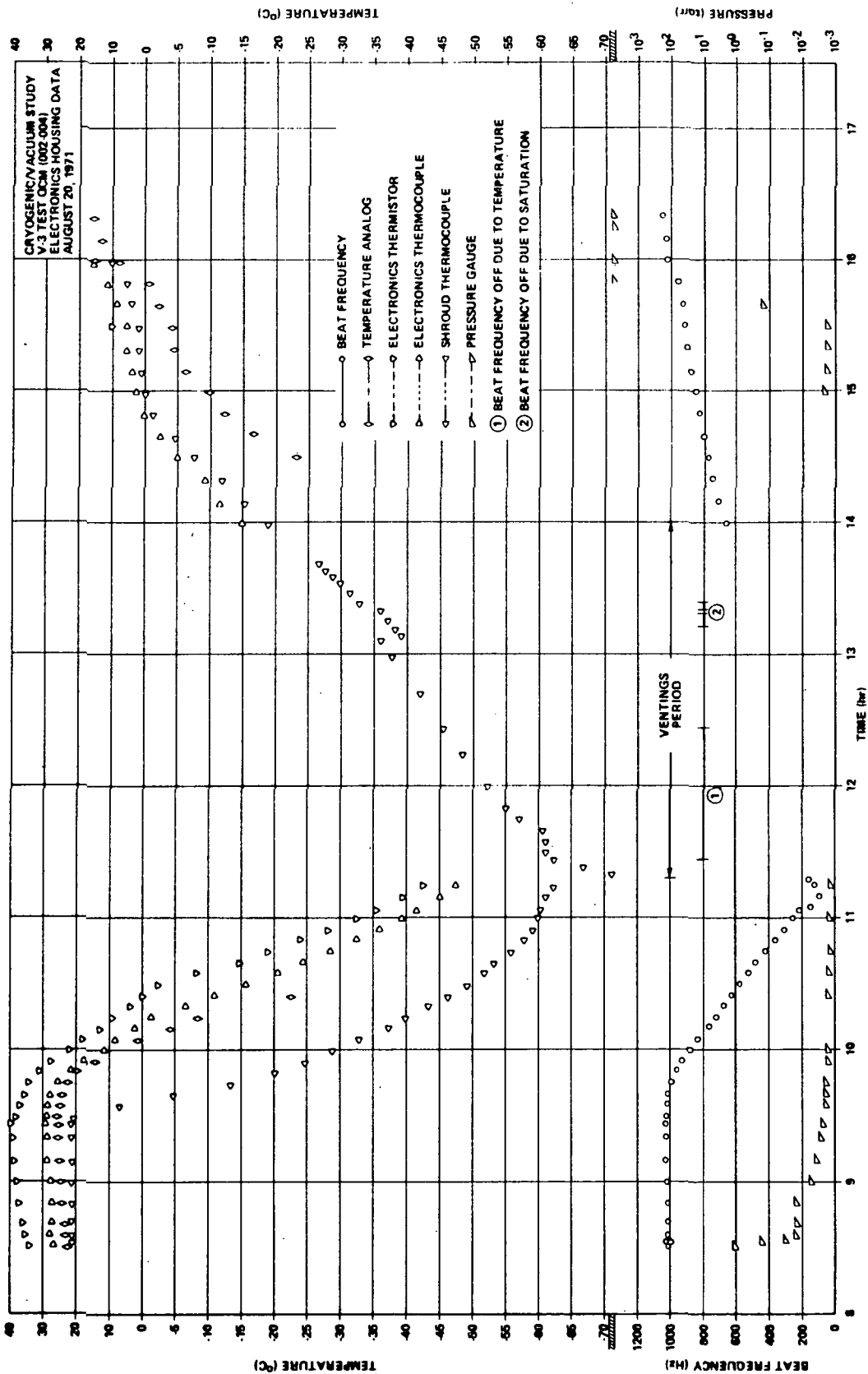


Figure 19. Cryogenic/vacuum study test data for QCM beat frequency, temperature analog, electronics housing thermistor, electronics housing thermocouple, shroud thermocouple, and chamber pressure as functions of time.

value, is presented in Table A-1 of the appendix. Using the thermal dependencies as plotted for known conversions and reasonable extrapolation, the calibration composite curves of Figure A-2 and A-3 of the appendix are presented. It is noted that these curves include representative manufacturer's-provided data for the temperature range above room temperature (see Figures A-4 and A-5 of the appendix, which are replotted to the same scale.) In Figure A-3, the significant difference in the curve trends is attributed to the QCM being a composite system as described earlier. The calibration curve (Fig. A-2) made the temperature scales of Figures 10 and 11 and Table A-2 possible.

The data reduction for the primary goal of analyzing the anomalous readings presented in Figures 10 and 11 is presented graphically in Figure 20. To assist in analyzing this graph, the significant events during the period are given in Table 2. The principal interpretive points were made by comparing the beat frequency behavior following time 1300 hrs to Figures 10 and 11.

IV. ANALYTICAL APPLICATION OF VACUUM STUDY TO V-3 TEST DATA

The conclusion for the anomalous readings in Figure 10 is that the variations represent deposition and reevolvement; i. e., data. To justify this, many factors must be examined. It is known [5,6] that during this time period of the V-3 Contamination Test, several chamber events occurred which could have impacted the QCM readings. At 0310 hrs, the seal oil trap high-temperature alarm was activated. This corresponds well with the pressure burst which evidently was associated with the QCM readings. However, at 0532 hrs, final verification was made that the trap unit had been functioning correctly. In addition, at 0314 hrs, gaseous molecular nitrogen was recorded as the predominant residual gas constituent of Chamber A. This is not necessarily unusual; however, the pressure burst in the chamber was later isolated to a gaseous nitrogen leak in the vicinity of the 5.79-m (19-ft) test stand. At 0335 hrs, a leak occurred in the MSFC Apollo Telescope Mount (ATM) gaseous nitrogen purge line, as determined by helium leak detection. This was corrected at 0455 hrs. Finally, heat transients were noted during the high vacuum heater calibration procedure for the ATM purge lines which would have sublimed quantities of atmospheric residuals such as nitrogen and water into the chamber environment. These heat transients occurred at 0334 hrs and 0540 hrs. These times correlated well with the start of the oscillations and the loss of beat frequency. Thus, there are two primary considerations.

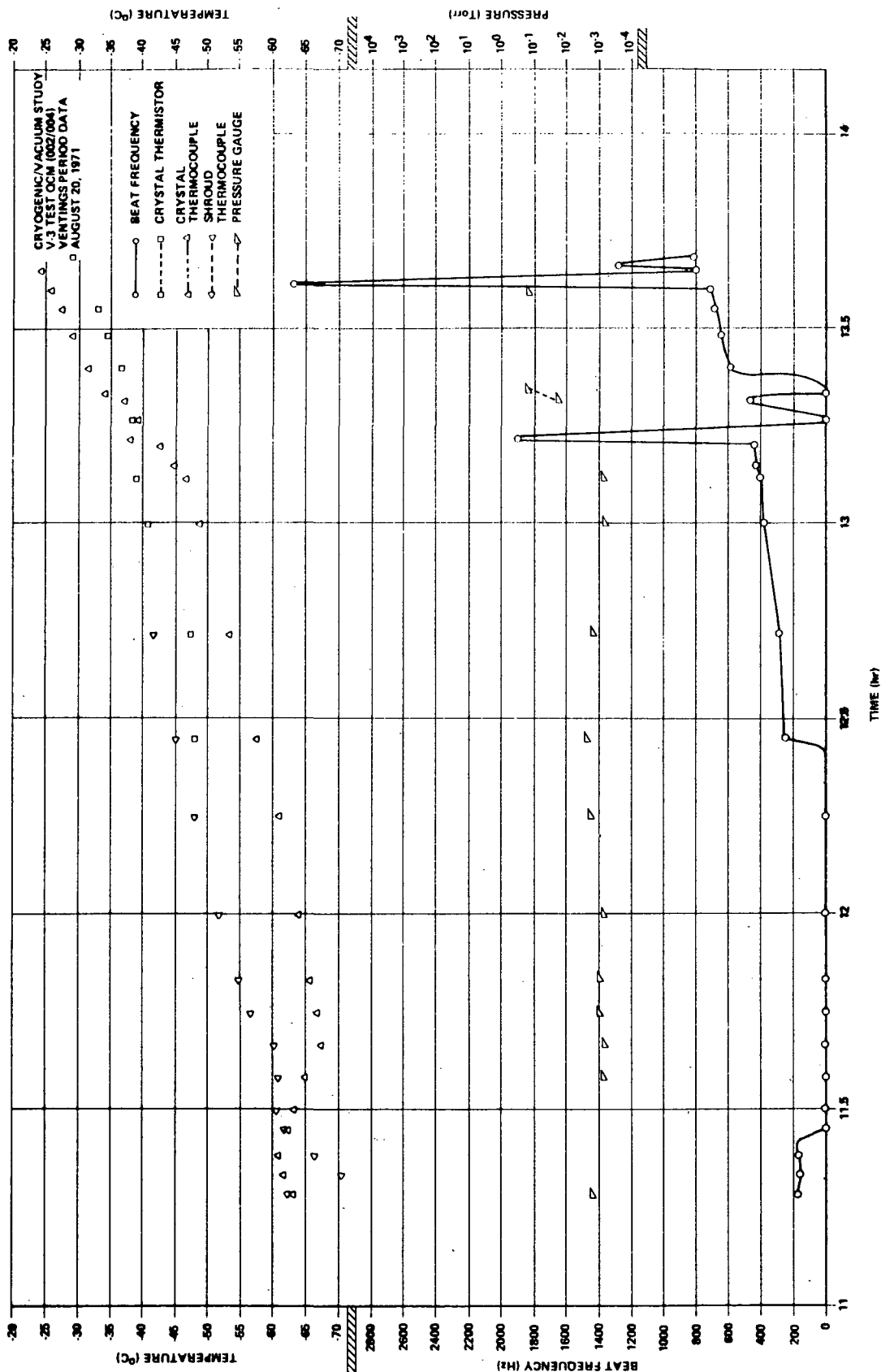


Figure 20. Cryogenic/vacuum study ventings test data for QCM beat frequency, temperature analog, shroud thermocouple, and chamber pressure as functions of time.

First, the heat transients caused thermal shift effects in the QCM readings. Second, the sources of water vapor and/or "wet" nitrogen caused the readings by deposition and reevolvment. The heat transients are believed not to have affected performance. This is based on the fact that the calibration procedure was terminated between 0334 hrs and 0540 hrs because of the heat transients. In addition, a comparison of Figures 10 and 11 shows that beat frequency thermal shifts are a few orders of magnitude less than those of the anomalous readings. A survey of chamber and test instrumentation operations for causes such as external noise sources was negative. Therefore, the analysis that the readings were caused by adsorption/desorption of water vapor and/or "wet" nitrogen, with saturation occurring just before 0600 hrs, will be assumed and tested.

The saturation concept is supported by the fact that at 0601 hrs and 0604 hrs, respectively, the solar arcs and infrared cage light and heat sources were turned on. The QCM readout functional pattern shows that these sources of energy caused the deposit to desorb, with the unit functioning correctly by 0630 hrs.

Consideration is now given to the results of the controlled environment test of the QCM unit as presented in Figures 18, 19, and 20. First, comparison of Figures 10, 18, and 19 shows that no electronics or crystal mismatch behavior patterns caused any oscillations like those of Figure 10. The only effect of simple cooling to cryogenic temperatures in a clean environment was to gradually and uniformly bring the beat frequency to zero. This occurs because of an effect on the QCM difference output common to all oscillator circuitry known as lockup. However, as shown in Figure 20 and Table 2, simple vents of water and/or "wet" air reproduced the behavior patterns of Figure 10. It is thus concluded that the QCM readings of Figure 10 are data representative of depositions. The composition of the deposits would likely be predominantly nitrogen and water.

The cause of the anomalous readout behavior as documented in Figure 11 is believed to be lockup of beat frequency. Again, to justify this, several factors must be examined. It is known [5, 6] that this information period covers the repressurization events for Chamber A. All pumping has been shut down, and at 0612 hrs the in-bleed of dry nitrogen has been started. However, the QCM readout pattern prior to and during this repressurization, up to 0624 hrs, follows a behavior pattern representing the temperature drop curve (Figs. 18 and A-3) rather than any deposition indications. The QCM unit also follows the temperature curve after the beat frequency returned (Fig. 9). The Boeing QCM readout did not show contamination level changes during this

period [6]. Finally, in the controlled environment test of the QCM unit, dry nitrogen or dry air vents at no time produced an effect resulting in saturation. Thus, since no deposition effects could be produced which simulated the data (Figs. 18 and 19) and since cryogenic cooldown can cause uniform decreases in beat frequency to lock up (Fig. A-3), the conclusion is that the cause of the behavior was beat frequency lockup caused by low temperature.

TABLE 2. SEQUENCE OF TEST EVENTS DURING THE VENTING PERIODS

Time	Event Description
11:09	Initiate blowout of LN ₂ from shroud
11:18	Individually initiate laboratory air vents to 200- μ peaks
11:19	
11:20	
11:21	
11:28	Initiate heat lamp to crystal housing side
11:36	Both thermistors (nos. 8 and 9) are off scale low
11:40	Moved heat lamp to directly view crystal housing
13:08	Individually initiate alcohol vents to 100- μ peaks
13:09	
13:13	Initiate water and water vapor vent to 200- μ peak
13:19	Initiate water vent, leaving isolation valve open
13:24	
13:27	Individually initiate laboratory air vents through "wetted" inlet chamber to 200- μ peaks
13:39	
13:40	

Because of the significant shifts in beat frequency of the QCM as a function of temperature alone in the limits of and outside of design ranges, it is concluded that calibration curves such as Figures A-2 and A-3 would be useful additions to instrument data packs. This is particularly recommended for experimenters intending to passively apply a QCM to flight measurements in which thermal patterns will likely be variable and uncontrollable.

A final recommendation is based on the comparison of Figures A-3 and A-5. Note the significant difference in actual performance of the composite system (002 crystal group and 004 electronics) and the separate performance curves. It is recommended that a controlled heating cycle behavioral test procedure be developed and be combined with the above cryogenic procedure to form a complete thermal range calibration technique. With empirical curves of this nature, extension of the curve-fitting and instrument constants¹ work would become possible for system composites not covered by acceptance test data.

1. MSFC memorandum (and revisions) entitled, "Constants to be Used in Data Analysis for QCMs on Skylab," by Dr. R. J. Naumann, dated May 27, 1971.

APPENDIX

REFERENCE INFORMATION, CHAMBER DATA
AND SUPPORTING TEST DATA

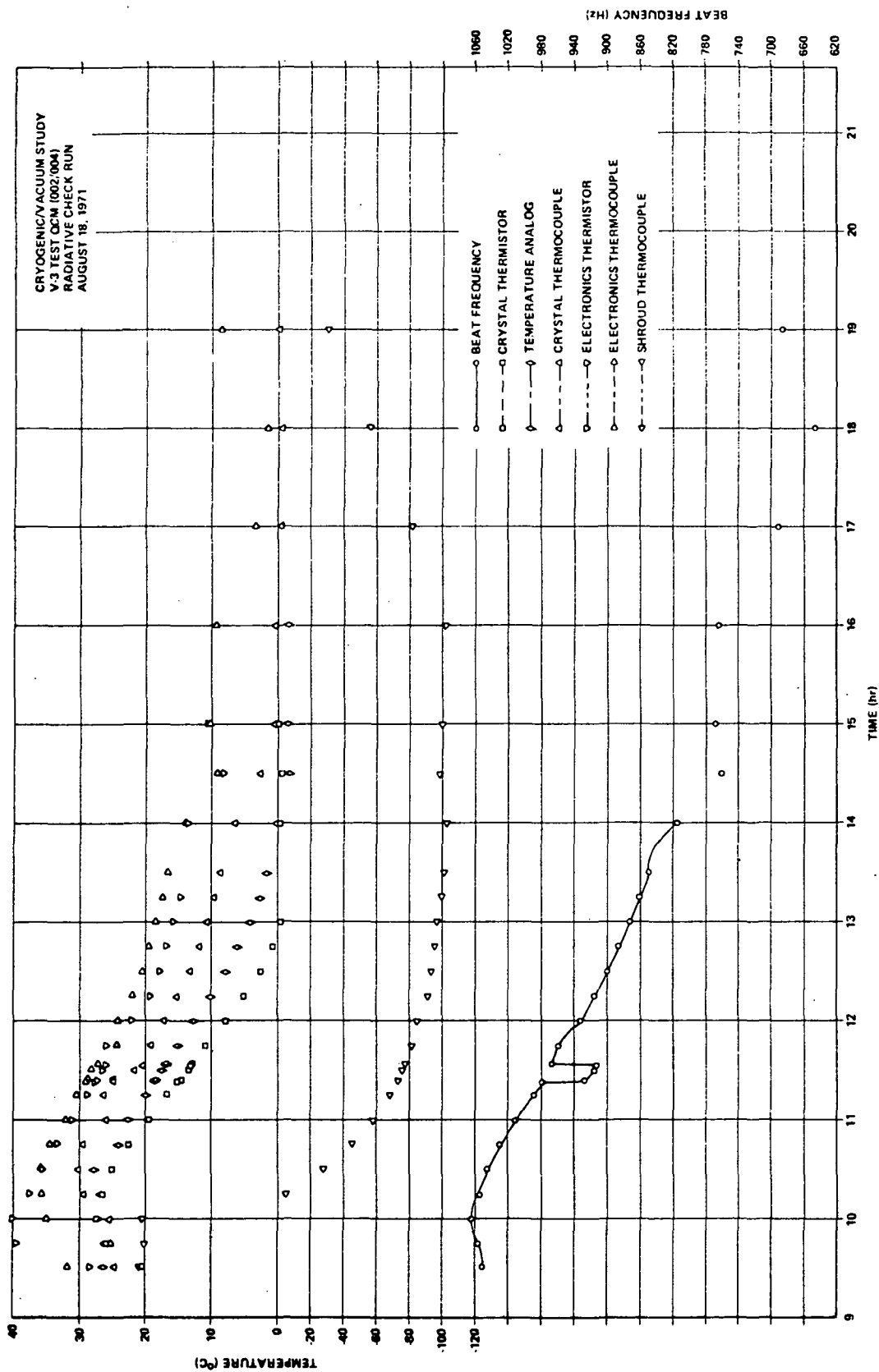


Figure A-1. Data graphical summary for the pre-test radiatively-cooled cryogenic/vacuum performance check.

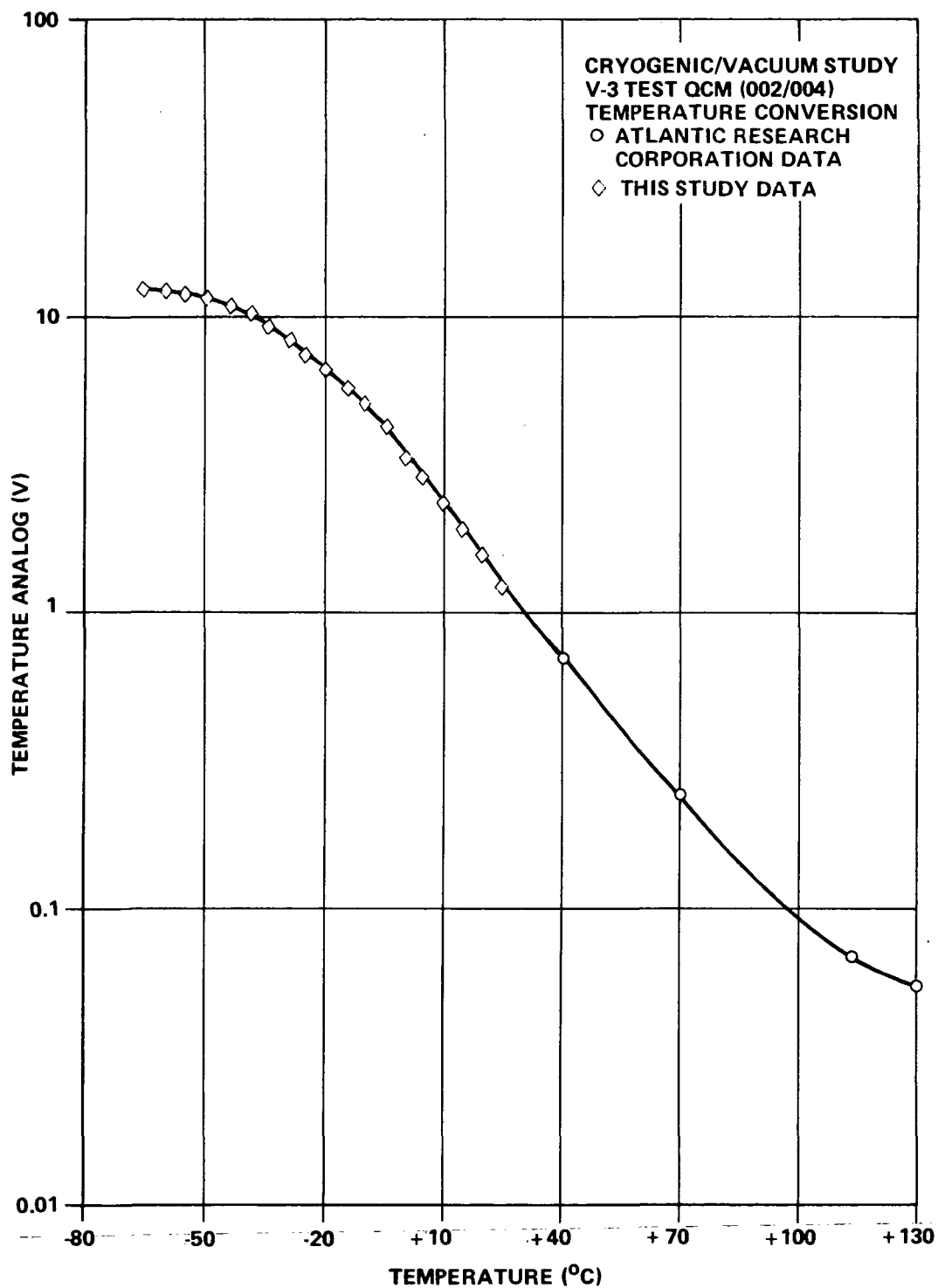


Figure A-2. Calibration curve for temperature analog voltage output versus temperature for the range +120° to -65°C.

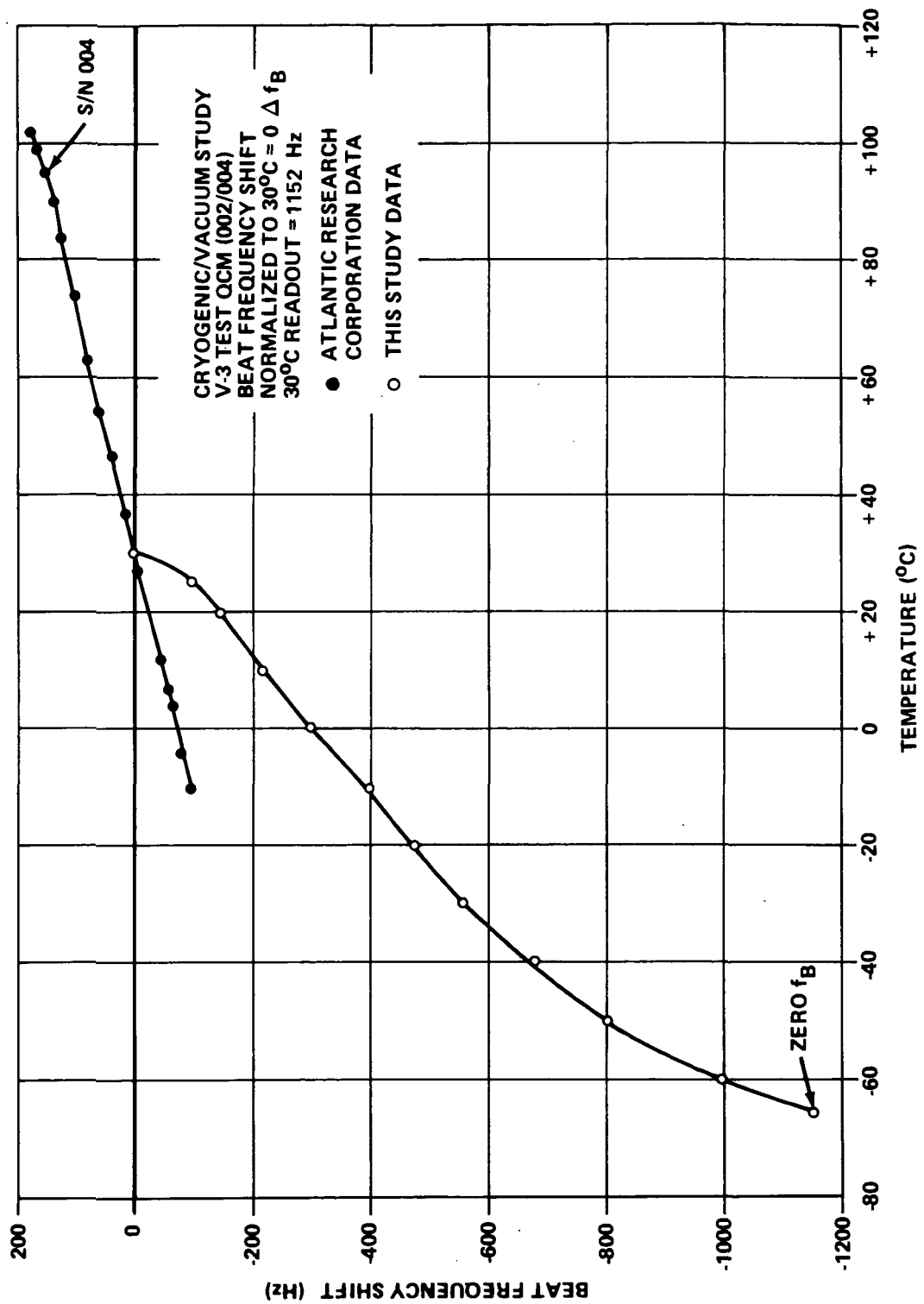


Figure A-3. Calibration curve for beat frequency output versus temperature for the range +120° to -65° C.

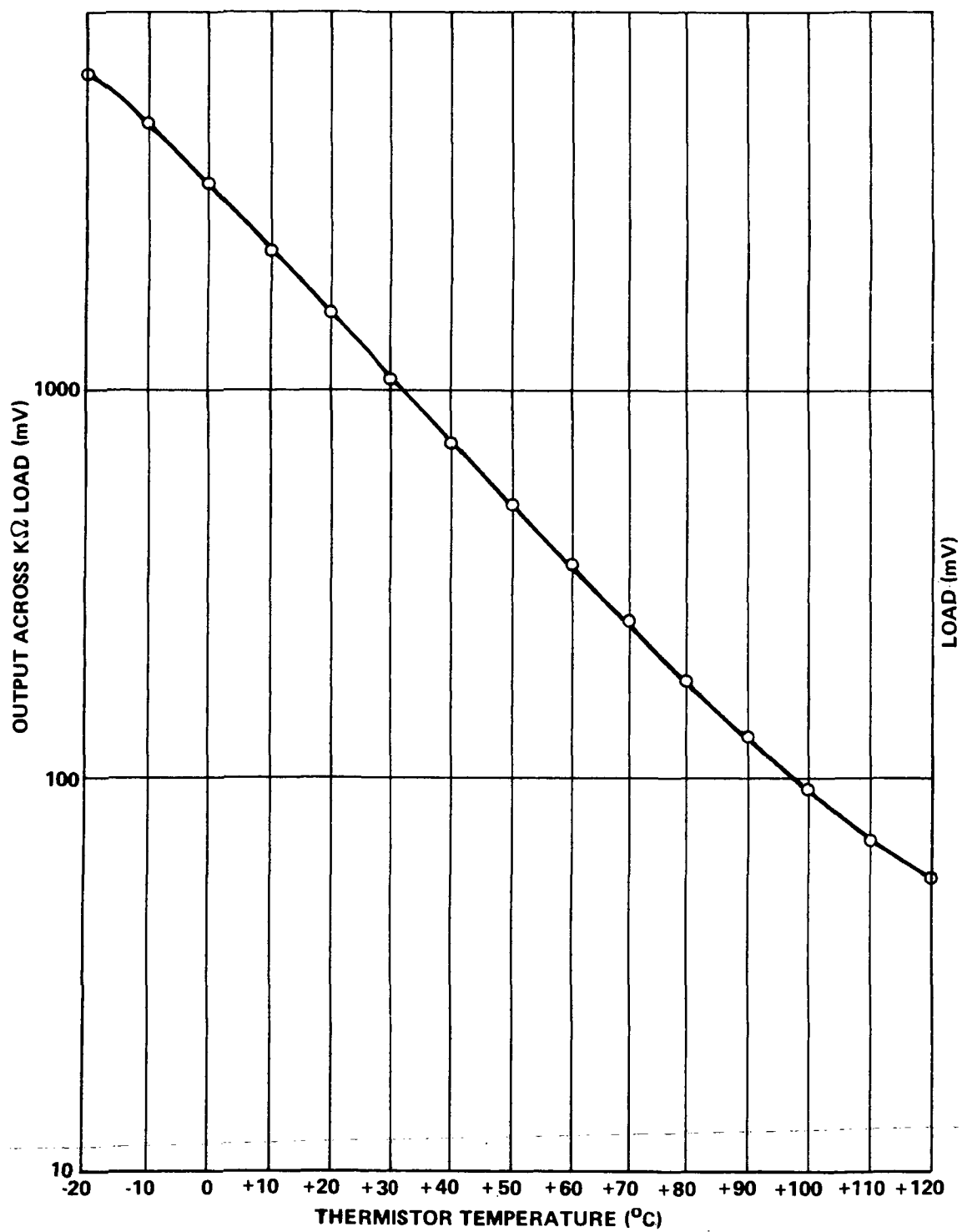


Figure A-4. Representative manufacturer (Atlantic Research Corporation) calibration curves for temperature analog shift thermal dependencies.

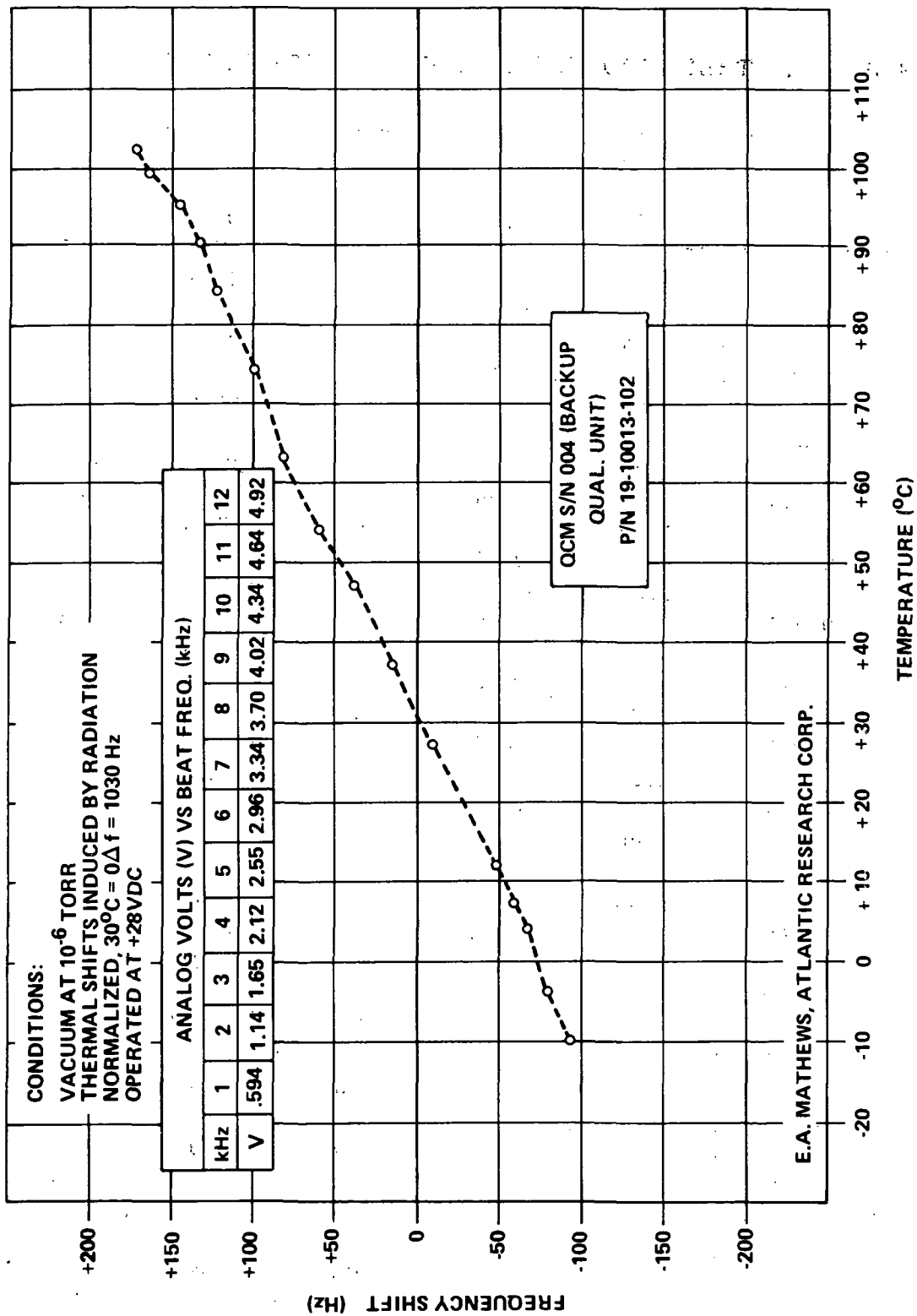


Figure A-5. Representative manufacturer (Atlantic Research Corporation) calibration curves for beat frequency shift thermal dependencies.

TABLE A-1. THERMOCOUPLE/THERMISTOR DATA CHART

Cu/Cn T/C (mV)	Δ (mV)	QCM T/M (V)	Δ (V)	Temp (°F)	Temp (°C)	Δ (°C)
-1.195		0.78		100	37.8	
	0.231		0.18			5.6
-1.426		0.96		90	32.2	
	0.228		0.19			5.6
-1.654		1.15		80	26.6	
	0.225		0.35			5.5
-1.879		1.50		70	21.1	
	0.223		0.40			5.5
-2.102		1.90		60	15.6	
	0.220		0.45			5.6
-2.322		2.35		50	10.0	
	0.217		0.50			5.6
-2.539		2.85		40	4.4	
	0.215		0.55			5.5
-2.754		3.50		30	-1.1	
	0.212		1.00			5.6
-2.966		4.50		20	-6.7	
	0.209		0.90			5.5
-3.175		5.40		10	-12.2	
	0.207		0.90			5.6
-3.382		6.30		0	-17.8	
	0.203		0.70			5.7
-3.585		7.00		-10	-23.5	
	0.200					5.4
-3.785				-20	-28.9	
	0.198					5.5
-3.983				-30	-34.4	
	0.194					5.6
-4.177				-40	-40.0	
	0.191					5.6
-4.368				-50	-45.6	
	0.187					5.5
-4.555				-60	-51.1	
	0.184					5.6

TABLE A-1 (Concluded)

Cu/Cn T/C (mV)	Δ (mV)	QCM T/M (V)	Δ (V)	Temp (° F)	Temp (° C)	Δ (° C)
-4.739	0.181			-70	-56.7	5.5
-4.920	0.177			-80	-62.2	5.6
-5.097	0.174			-90	-67.8	5.5
-5.271	0.171			-100	-73.3	5.6
-5.442	0.168			-110	-78.9	5.5
-5.610	0.164			-120	-84.4	5.6
-5.774	0.160			-130	-90.0	5.6
-5.934	0.157			-140	-95.6	5.5
-6.091	0.153			-150	-101.1	5.6
-6.244				-160	-106.7	

TABLE A-2. TEMPERATURE ANALOG CONVERSION DATA

QCM T/M (V) ^a	Δ (V)	Temp (° F)	Δ (° F)	Temp (° C)	Δ (° C)	QCM T/M (V) ^b	Δ (V)
0.73		104		40			
	0.12		9		5		
0.85		95		35			
	0.22		9		5		
1.07		86		30			
	0.21		9		5		
1.28		77		25		1.246	
	0.30		9		5		0.340
1.58		68		20		1.586	
	0.35		9		5		0.410
1.93		59		15		1.996	
	0.42		9		5		0.371
2.35		50		10		2.367	
	0.51		9		5		0.458
2.86		41		5		2.825	
	0.59		9		5		0.545
3.45		32		0		3.370	
	0.65		9		5		0.991
4.10		23		-5		4.361	
	0.90		9		5		0.713
5.00		14		-10		5.074	
	0.80		9		5		0.667
5.80		5		-15		5.741	
	0.90		9		5		0.864
6.70		-4		-20		6.605	
			9		5		0.769
		-13		-25		7.374	
			9		5		0.916
		-22		-30		8.290	
			9		5		0.999
		-31		-35		9.289	
			9		5		0.965
		-40		-40		10.254	
			9		5		0.898

TABLE A-2. (Concluded)

QCM T/M (V) ^a	Δ (V)	Temp (°F)	Δ (°F)	Temp (°C)	Δ (°C)	QCM T/M (V) ^b	Δ (V)
		-49		-45		11.152	
			9		5		0.582
		-58		-50		11.734	
			9		5		0.530
		-67		-55		12.264	
			9		5		0.386
		-76		-60		12.650	
			9		5		0.300
		-85		-65		12.950	
			.9		.5		0.012
		-85.9		-65.5		12.962	

a. Atlantic Research Corporation calibration (Fig. A-4).

b. Data from this study.

REFERENCES

1. Moore, W. Walding, Jr., and Tashbar, Philip W.: A Custom System for Measuring Optical Effects of Aerospace Materials Contamination Deposits. J. of Contamination Control, March 1971.
2. Lunar Excursion Module RCS Engine Vacuum Chamber Contamination Study. Gary M. Arnett, Technical Coordinator, NASA TM X-53859, July 8, 1969.
3. Operational Plan for the Quartz Crystal Microbalance on the T-027 Sample Array, the ATM, and the EREP. TM-015-002-2H, MSFC, April 19, 1971.
4. Operational Plan in Support of the V-3 Contamination Test, the ATM Thermal Vacuum Test, and the ATM Calibration Test in MSC's Chamber A, Revision A. TM-015-001-24, MSFC, February 1, 1971.
5. Space Environment Simulation Lab; Test Director Event Log; V-3 Contamination Test, No. 33-A-71, MSC.
6. Space Environment Simulation Lab; Standard Operating Procedure Checklist and Event Log; V-3 Contamination Test, No. 33-A-71, MSC.

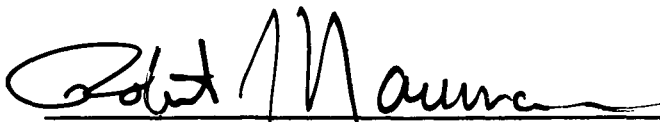
APPROVAL

THE V-3 CONTAMINATION TEST OF THE CHAMBER A FACILITY AND A SUBSEQUENT CRYOGENIC/VACUUM STUDY OF THE V-3 TEST QUARTZ CRYSTAL MICROBALANCE

By W. Walding Moore, Jr., and Philip W. Tashbar

The information in this report has been reviewed for security classification. Review of any information concerning Department of Defense or Atomic Energy Commission programs has been made by the MSFC Security Classification Officer. This report, in its entirety, has been determined to be unclassified.

This document has also been reviewed and approved for technical accuracy.



ROBERT J. NAUMANN

Chief, Physics and Astrophysics Division



CHARLES A. LUNDQUIST

Director, Space Sciences Laboratory

DISTRIBUTION

<u>INTERNAL</u>	<u>INTERNAL (Concluded)</u>	<u>EXTERNAL (Continued)</u>	<u>EXTERNAL (Concluded)</u>
DIR Dr. R. Petrone	S&E-AERO-DIR Dr. E. Geissler	NASA Headquarters Washington, D. C. 20546 Attn: Mr. William Schneider - ML Mr. P. E. Culbertson - MT Mr. D. L. Forsythe - MLA Dr. L. N. Werner - MLA Dr. John E. Naugle - S Mr. Jesse L. Mitchell - SG Mr. J. M. Weldon - SG Mr. Maurice Dubin - SG Mr. R. E. Halpern - SG Mr. Henry J. Smith - SS Dr. G. Oertel - SG Dr. Nancy G. Roman - SG Mr. R. Chase - SG Mr. B. T. Lundin - R Mr. N. P. Fransden - RB Mr. R. D. Ginter - RF Dr. H. H. Kurzweg - RRP Mr. D. Novik - RFE Mr. H. L. Anderton - REG Dr. R. Nash - RRT Mr. J. Maltz - RWM	Goddard Space Flight Center Greenbelt, Maryland 20771 Attn: Mr. H. Shapiro - 322 Dr. F. Paul - 327
DEP	S&E-ASTR-DIR Mr. Brooks Moore Mr. W. P. Horton	Naval Research Laboratory Washington, D. C. 20390 Attn: Dr. Richard Tousey - 7140-137 Dr. G. Carruthers - 7126-10 Dr. T. C. Winter, Jr. - 7140W Mr. W. R. Hunter - 7143	
AD-S Dr. Ernst Stuhlinger Dr. George Bucher	S&E-ASTN-DIR Mr. K. Heimburg		
A&PS-PAT Mr. L. D. Wofford, Jr.	S&E-ASTN-M Mr. R. Schwinghamer Mr. J. Horton Mr. C. Smith		
A&PS-MS-H A&PS-MS-IP (2) A&PS-MS-IL (8) A&PS-TU (6)	S&E-QUAL-E Mr. E. Buhmann		High Altitude Observatory P. O. Box 1558 Boulder, Colorado 80302 Attn: Dr. Gordon Newkirk, Jr.
PA Mr. D. Newby	S&E-QUAL-PSI Mr. Max Rosenthal		Ball Brothers Research Corporation P. O. Box 1062 Boulder, Colorado 80302 Attn: Mr. H. C. Poehlmann Mr. D. A. Toalstad Mr. J. Austin Dr. R. Herring
S&E-DIR Dr. H. K. Weidner Mr. L. G. Richard	S&E-QUAL-OCM Mr. E. Davis	Johnson Space Center Houston, Texas 77058 Attn: Dr. O. G. Smith - KW Mr. J. A. Smith, Jr. - ES3 Mr. J. T. Taylor - ES3 Mr. A. McIntyre - EL3 Mr. F. U. Williams - EL2 Mr. W. K. Roberts - BD2 Mr. J. Visentine - EL3 Dr. E. G. Gibson - CB Mr. G. P. Donner - TN23 Mr. B. R. Warden - KS	Hayes International Corporation P. O. Box 1568 Huntsville, Alabama 35807 Attn: Mr. William T. Weissinger
S&E-R-DIR Dr. W. G. Johnson	S&E-SSL-DIR Dr. C. Lundquist Mr. R. Hembree		
S&E-P-DIR Mr. H. Kroeger	S&E-SSL-X Dr. J. Dozler Mr. H. Weathers		
S&E-SSL-P Dr. R. Naumann Mr. R. L. Holland Mr. E. Klingman Mr. J. McGuire Mr. W. Moore (25) Mr. J. Williams	S&E-SSL-N Dr. R. Decher Mr. H. Stern Dr. T. Parnell Dr. A. deLoach Mr. M. Burrell		
S&E-SSL-S Dr. W. H. Sieber Mr. G. Loughhead	PD-CVT Mr. W. Brooksbank		
S&E-SSL-T Mr. W. Snoddy Mr. E. Miller Mr. G. Arnett Mr. B. Jones Mr. J. Reynolds Mr. R. Linton Mr. J. Zwiener	MO-MGF Mr. H. F. Kurtz		
S&E-SSL-C Reserve (5)	MO-I Mr. H. Golden		
PD-DIR Mr. J. Murphy	SL-MGR Mr. L. Belew		
PD-MP Mr. H. Gierow Mr. H. Dudley Mr. R. Potter	SL-DP Mr. J. Waite		
PD-AP Mr. J. Downey	SL/SE-ATM Mr. R. Ise Mr. W. Keathley Mr. J. Igou Mr. D. E. Spoddy Mr. E. Cagle Mr. A. White Mr. E. R. Cantrell		
	<u>EXTERNAL</u> Scientific and Technical Information Facility (25) P. O. Box 33 College Park, Maryland 20740 Attn: NASA Representative (S-AK/RKT)		
		Martin-Marietta Denver, Colorado 80201 Attn: Mr. R. Sawyer Dr. Muscari Mr. J. Wade Dr. Mangold Mr. Anthony	
		The Boeing Company Seattle, Washington 98110 Attn: Dr. W. A. Eul Mr. Roger Gillette	
		General Electric Company Valley Forge Technology Center P. O. Box 8555 Philadelphia, Pa. 19101 Attn: Mr. J. Scannapieco	
		Kennedy Space Center Kennedy Space Center, Florida 32899 Attn: Mr. R. A. Bland - AA-SVO-3	
		Langley Research Center Langley Station Hampton, Virginia 23665 Attn: Mr. J. P. Mugler, Jr. - MS-214 Mr. E. L. Hoffman - 188A	
		Ames Research Center Moffett Field, California 94035 Attn: Mr. E. R. Streed Vehicle Systems Design Branch	